POLITECNICO DI TORINO

Collegio di Ingegneria Chimica e dei Materiali

Corso di Laurea Magistrale
in Ingegneria dei Materiali

Tesi di Laurea Magistrale

Characterization of Block copolymers thin films

Relatori:
Prof. Marco Sangermano
Prof. Galder Kortaberria Altzerreka

Candidato:
Andrea Richiardone

Dicembre 2019

Sommario

1 Caratterizzazione di copolimeri a blocchi in forma di film sottili 1

2 Introduction 17

2.1 Block Copolymers 17

2.2 Block copolymers in bulk 18

2.3 Block copolymers thin films 20

2.4 Self-assembly in thin films 20

2.5 Annealing techniques 23

2.5.1 Thermal Annealing 24

2.5.2 Solvent Vapour annealing (SVA) 25

2.6 Nanostructured morphologies 27

2.6.1 Lamellar morphology 27

2.6.2 Hexagonally packed cylinders morphology 27

2.6.3 Gyroid morphology 27

2.6.4 Spherical morphology 28

2.7 Applications 28

3 Materials and methods 31

3.1 Block copolymers 31

3.1.1 PS-b-P4VP 31

3.1.2 PS-b-PMMA 31

3.1.3 PS-b-PCL 32

3.2 Films preparation 32

3.2.1 Solutions Preparation 33

3.2.2 Substrate Preparation 34

3.2.3 Spin Coating Process 34

3.2.4 Annealing treatments 36

3.3 Experimental techniques 37

3.3.1 Thermal analysis 37

3.3.2 Morphological analysis by AFM 39

4 Results and discussion 41

4.1 Thermal analysis 41

4.1.1 PS-bP4VP 41

4.1.2 PS-b-PMMA 43

4.1.3 PS-b-PCL 45

4.2 AFM 47

4.2.1 PS-b-P4VP 47

4.2.2 PS-b-PMMA 48
4.2.3 PS-b-PCL 49
5 Conclusions 50
6 References 51

1 CARATTERIZZAZIONE DI COPOLIMERI A BLOCCHI IN FORMA DI FILM SOTTILI

Introduzione

I copolimeri a bocchi sono una particolare tipologia di polimeri composti da due o più unità monomeriche differenti, le quali si ripetono in maniera ordinata secondo una disposizione del tipo AAA-BBB (nel caso di un copolimero a due blocchi) come in figura.

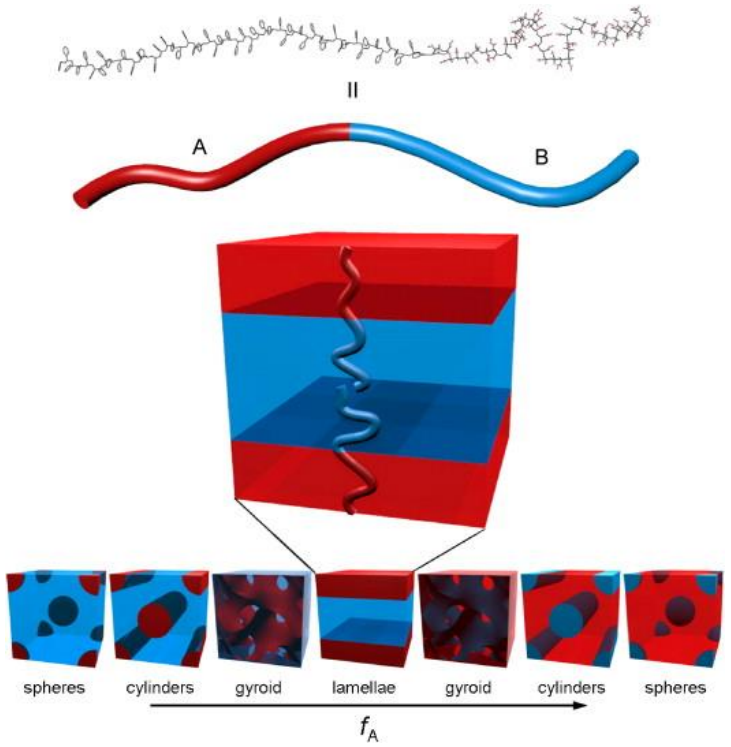

Figra 1.1. Alcune morfologie stabili di un generico copolimero a due blocchi

La peculiarità di questa classe di polimeri risiede nel fatto che le unità monomeriche non solo risultano differenti dal punto di vista della composizione chimica, ma risultano anche incompatibili dal punto di vista elettrostatico: i due blocchi sono infatti uno idrofilo e l'altro idrofobo tuttavia, essendo legati da un legame covalente, essi non possono separarsi; per cui il materiale risulta bifasico a livello microscopico. Questa separazione di fase, come verrà spiegato più avanti, può essere controllata, per cui risulta possibile ottenere materiali nanostrutturati, ovvero aventi una struttura ordinata e ben controllabile con precisione su scala nanomentrica. Queste strutture evolvono spontaneamente da una disposizione casuale (random coil) a una morfologia ordinata, per cui tale fenomeno prende il nome di autoassemblaggio. Dal lavoro sperimentale effettuato finora risulta possibile modificare la struttura di questa classe di polimeri attraverso il controllo della composizione (percentuale in massa di ciascun blocco) e di alcuni parametri operativi come temperatura e atmosfera. In quest'affermazione risiede lo scopo di questo lavoro, ovvero la

caratterizzazione di tali materiali, al fine di meglio comprendere i meccanismi che ne governano l'evoluzione morfologica e poterne quindi meglio controllare il processo di autoassemblaggio. In questo modo è possibile ottenere materiali aventi le più svariate proprietà, con un vasto campo di applicazioni, dalla litografia in microelettronica, allo sviluppo di celle solari di nuova generazione, passando per dispositivi ottici e medici all'avanguardia.

Siccome il fenomeno dell'autoassemblaggio dipende da molti fattori, al fine di riuscire ad effettuare un'analisi il più possibile precisa, durante questo lavoro si sono analizzati questa classe di materiali nella sola forma di film sottili. Nello specifico sono stati analizzati tre copolimeri simmetrici lineari composti da due blocchi, tutti di origine commerciale (PS b P4VP, PS b PMMA, PS b PCL).

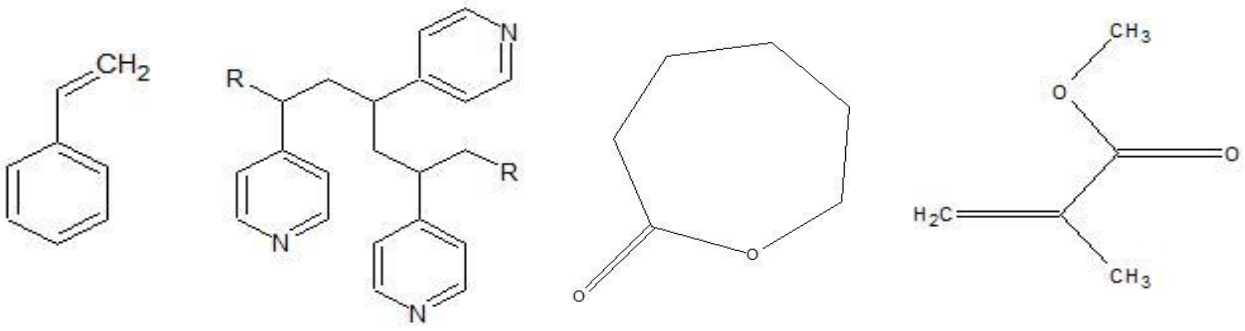

Figura 1.2. Monomeri dei diversi blocchi utilizzati: stirene,
4-vinilpiridina, metilmetacrilato, caprolattona (da sx a dx rispettivamente)

Per ottenere film sottili è necessario sciogliere il polimero (commercializzato sotto forma di polvere) in un solvente adeguato. In tal senso sono stati calcolati i vari parametri di solubilità di Flory (χ) i quali, seguendo il modello proposto da Flory ed Huggins, danno un'indicazione sull'affinità di ciascun blocco con i diversi solventi. Secondo la letteratura, essi risultano essere buoni solventi per un determinato blocco nel caso in cui risulti $\chi \leq 0.5$.

	H_2O	EtOH	TOLUENE	ACETONE	DMF	DIOXANE	THF
χ_{PS}	4,817	0,377	0,684	0,157	0,212	0,100	0,448
χ_{P4VP}	4,522	0,241	0,985	0,285	0,102	0,216	0,662
χ_{PMMA}	6,091	1,222	0,027	0,024	1,056	0,078	0,008
χ_{PCL}	6,007	1,155	0,043	0,015	0,984	0,058	0,016

Tabella 1.1. Valori del parametro di Flory per i diversi polimeri
Al variare del solvente

In accordo con la letteratura, sono stati scelti come solventi la DMF, il THF e il toluene per sciogliere PS b P4VP, PS b PMMA e PS b PCL rispettivamente. Per il lavoro sperimentale si è partiti dalla pesata delle polveri di polimero, in seguito sono state calcolate le quantità di solvente necessario ad ottenere soluzioni aventi determinate concentrazioni, anch'esse ricavate dalla letteratura. Nei casi analizzati si è mantenuta una concentrazione pari al 1% in massa. Siccome l'analisi morfologica viene realizzata tramite la microscopia a forza atomica (AFM) si è resa necessaria la realizzazione di campioni (film) dallo spessore più omogeneo possibile. A tale scopo si è scelta la tecnica dello spin coating per ottenere i film adatti. Come substrato è stato utilizzato vetro da laboratorio, sul quale è stata depositata una singola goccia per ciascun campione. È stato utilizzato poi uno spin coater P6700 da specialty coating systems

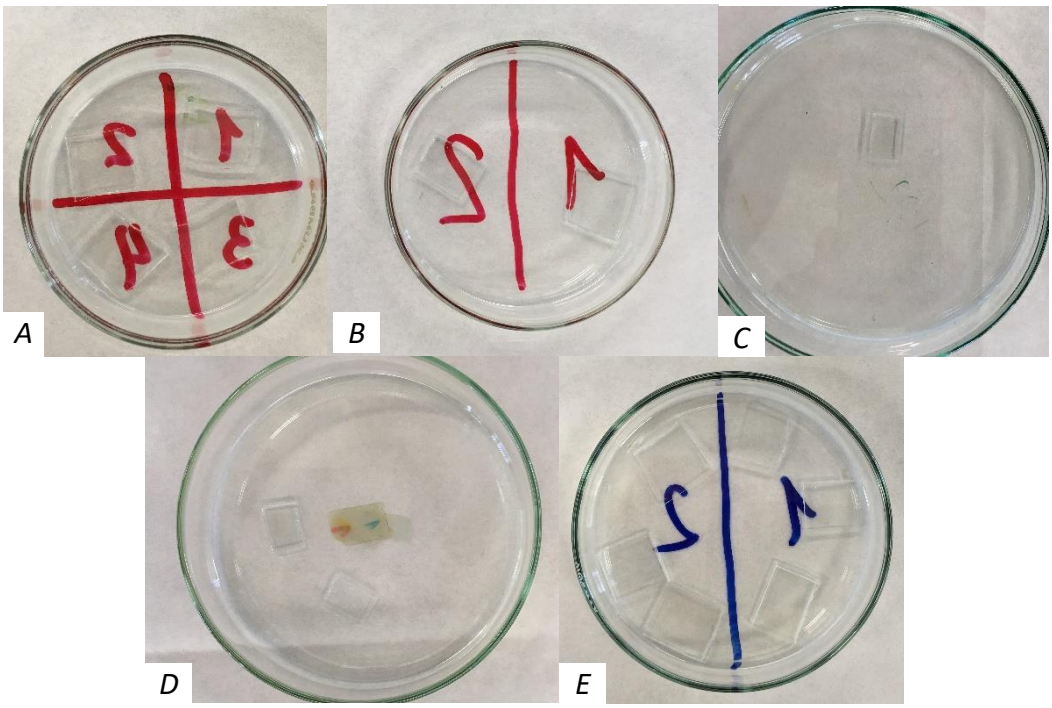

Figura 1.3. Campioni di film su substrato di vetro da laboratorio, ottenuti tramite spin coating

per 120 s alla velocità di rotazione di 2000 rpm, tramite il quale i tempi di allontanamento del solvente sono stati notevolmente diminuiti; inoltre ha reso possibile ottenere campioni dallo spessore più omogeneo. Al termine di questi processi i campioni appaiono come in figura 1.3.

Una volta ottenuti i film si è passati allo step successivo, ovvero al processo di invecchiamento (annealing), durante il quale si verifica il fenomeno di autoassemblaggio. Durante questa fase la mobilità delle catene polimeriche risulta di fondamentale importanza, perché solo nel caso in cui possiedano sufficiente mobilità esse potranno disporsi secondo una struttura ordinata; evolvendo verso una situazione di equilibrio termodinamico. In questo stato infatti le principali forze in

gioco (repulsione chimica e minimizzazione delle interfacce) si bilanciano. Per fornire la sufficiente mobilità alle macromolecole, sono state scelte due differenti tecniche: l'invecchiamento termico (thermal annealing) e l'invecchiamento in atmosfera controllata (solvent vapour annealing). I campioni di PS b PCL sono stati sottoposti a thermal annealing in un forno sottovuoto uno a 120°C e l'altro a 100°C.

Figura 1.4. Forno per invecchiamento termico con campioni all'interno

I campioni di PS b PMMA e PS b P4VP invece sono stati invecchiati in vapori di acetone e diossano rispettivamente. Per entrambi i polimeri sottoposti al trattamento di SVA sono stati preparati due diversi campioni, utilizzati per tempi di esposizione differenti di 24 e 48 ore.

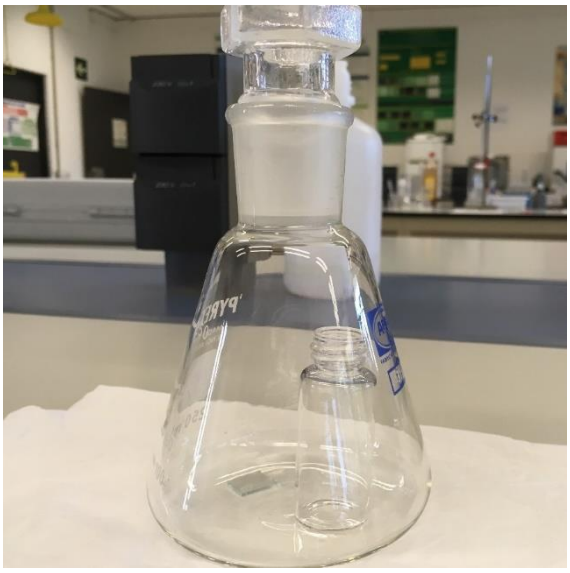

Figura 1.5. Set up per il processo di solvent vapour annealing (SVA)

A questo punto si è passati alla caratterizzazione dei film ottenuti: come prove sono state scelte prima le analisi termiche (DSC e TGA) e successivamente l'analisi per immagini delle strutturee ottenute tramite AFM. Per le analisi termiche si è utilizzato lo strumento fornito da Mettler Toledo TGA/DSC3+; nello specifico la TGA è stata svolta in un intervallo di temperatura compreso tra T_{amb} e 600°C per il PS b PMMA e T_{amb} e 800°C per i campioni di PS b P4VP e PS b PCL. Per tutti i campioni si è scelta una velocità di riscaldamento pari a 10°C/min. La scelta di questi parametri è stata fatta in accordo con la letteratura e la pratica del laboratorio. Per quanto riguarda la DSC, è stato utilizzato lo stesso strumento impostato con la stessa velocità di riscaldamento, mentre l'intervallo di temperatura è stato ridotto da T_{amb} a 200°C. Per essere sicuri dell'affidabilità dei risultati ottenuti con la DSC si è deciso di effettuare una rampa di riscaldamento preliminare, seguita da un raffreddamento e da un secondo riscaldamento. Nei termogrammi mostrati in seguito verrà mostrato il grafico relativo al solo secondo riscaldamento, essendo esso quello più rappresentativo; poiché relativo al campione privo di umidità.

Figura1.6. Apparecchiatura per le analisi termiche (Mettler Toledo TGA/DSC3+)

Sempre per quanto riguarda la DSC lo strumento opera in modalità flusso di calore; per cui il campione di riferimento e quello di prova si trovano nella stessa camera. Partendo dalla differenza di T presente tra i due, si ricava il calore che vi fluisce attraverso un ponte termico (il supporto, del quale si conosce la resistenza termica). Tale principio si basa sulla legge di Ohm:

$$\dot{Q} = \frac{\Delta T}{R}$$

Della quale si conosce il ΔT misurato dalle termocoppie, mentre la resistenza è una proprietà del materiale.

Per l'analisi morfologica si è scelto di utilizzare l'AFM: con questa tecnica, che si basa sull'interazione tra gli atomi della punta dello strumento e gli atomi della superficie del campione, è possibile ottenere informazioni molto dettagliate riguardo la morfologia della superficie. Per questa analisi è stata usata una sonda ICON di Bruker, operante in tapping mode (TM-AFM). La punta integrata in silicio proviene dallo stesso produttore, e possiede una frequenza di risonanza intorno ai 300kHz. La misura è stata effettuata a una velocità di scansione di 1 Hz/s con 512 linee di scansione. La scelta di utilizzare la sonda in tapping mode è nata poiché risulta il miglior compromesso tra risoluzione e precisione della microscopia, senza rischiare di danneggiare la superficie del film o la sonda stessa.

Discussione dei risultati

Analisi termiche

PS-b-P4VP

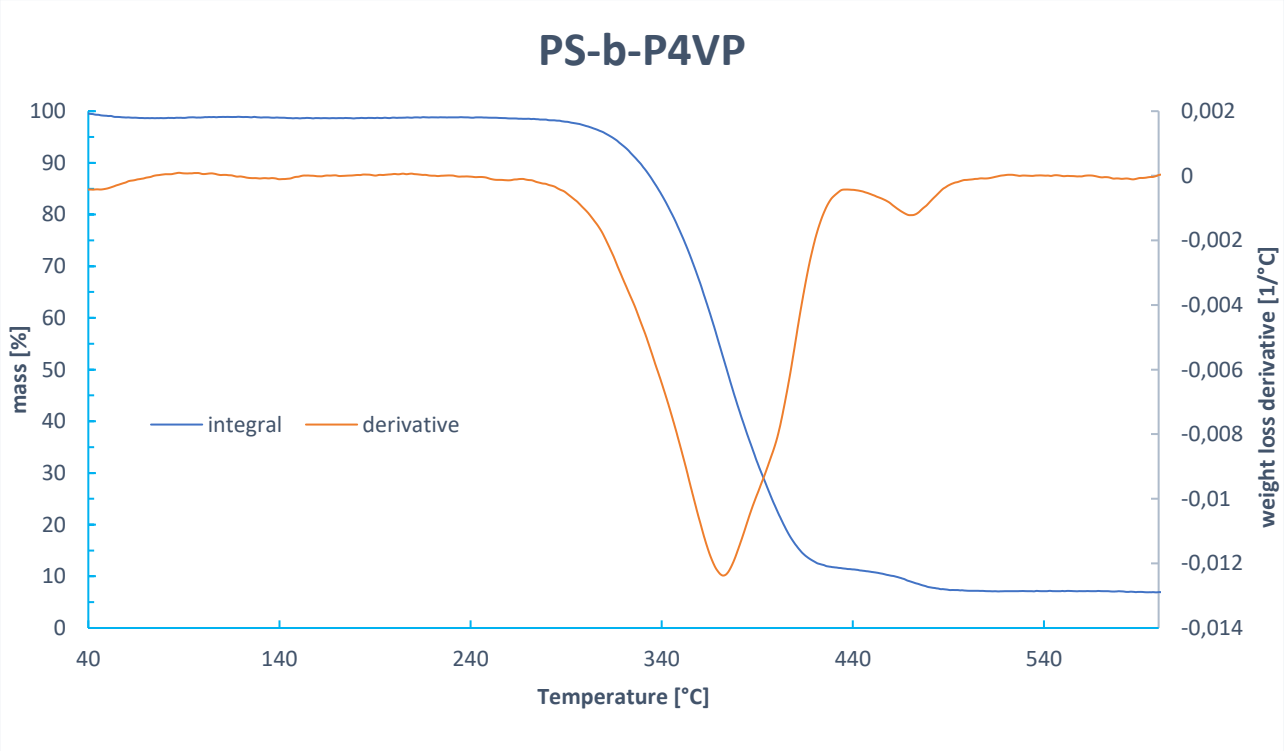

Figura 1.7. TGA PS b P4VP

Durante la TGA sono stati usati 1.4038 mg di polimero. Come si può notare dalla figura la degradazione termica avviene in due step: ciò si nota soprattutto grazie alla curva derivata, la quale presenta due picchi ben distinti (i quali si riferiscono ad un massimo della velocità di degradazione) intorno a 475°C e 375°C. Questo comportamento può

essere interpretato, in accordo con quanto trovato in letteratura, come la conseguenza della differente resistenza termica dei due blocchi, la cui temperatura alla quale si osserva la massima velocità di degradazione risulta essere intorno a 430°C per il PS (M_n=8000) e 400°C per la P4VP (M_n=13000). Per questo motivo si potrebbe assegnare il primo step di degradazione (quello intorno ai 375°C) al blocco di P4VP mentre quello a temperatura maggiore potrebbe essere dovuto alla degradazione del blocco stirenico.

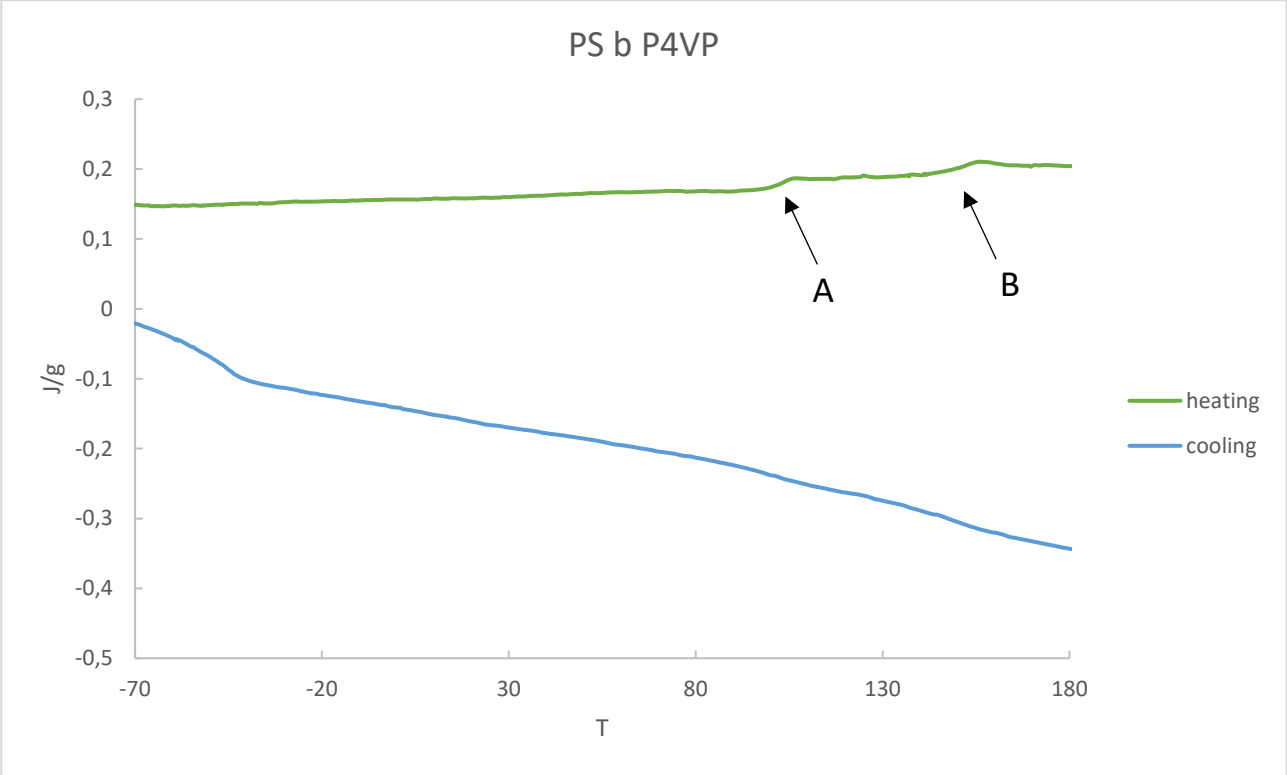

Figura 1.8. Termogrammi DSC per PS b P4VP

Per l'analisi DSC sono stati utilizzati 2.033 mg di polimero. Dal termogramma non si nota alcun picco (il quale sarebbe dovuto ad ev. cristallizzazioni o fusioni), per cui è possibile supporre che il copolimero sia amorfo. Tale teoria è confermata dalla presenza di due flessi (A e B in figura), i quali indicano la presenza di due temperature di transizione vetrosa (T_g) rispettivamente a 104°C e 149°C. L'ipotesi risulta plausibile e in accordo con la letteratura, in quanto le T_g di PS e P4VP risultano essere rispettivamente intorno a 100°Ce 150°C.Inoltre, la presenza di due differenti transizioni vetrose indica una separazione di fase del campione, il che risulta una prova della separazione di fase che è avvenuta a livello microscopico (microphase separation), tipica dei copolimeri autoassemblanti.

PS-b-PMMA

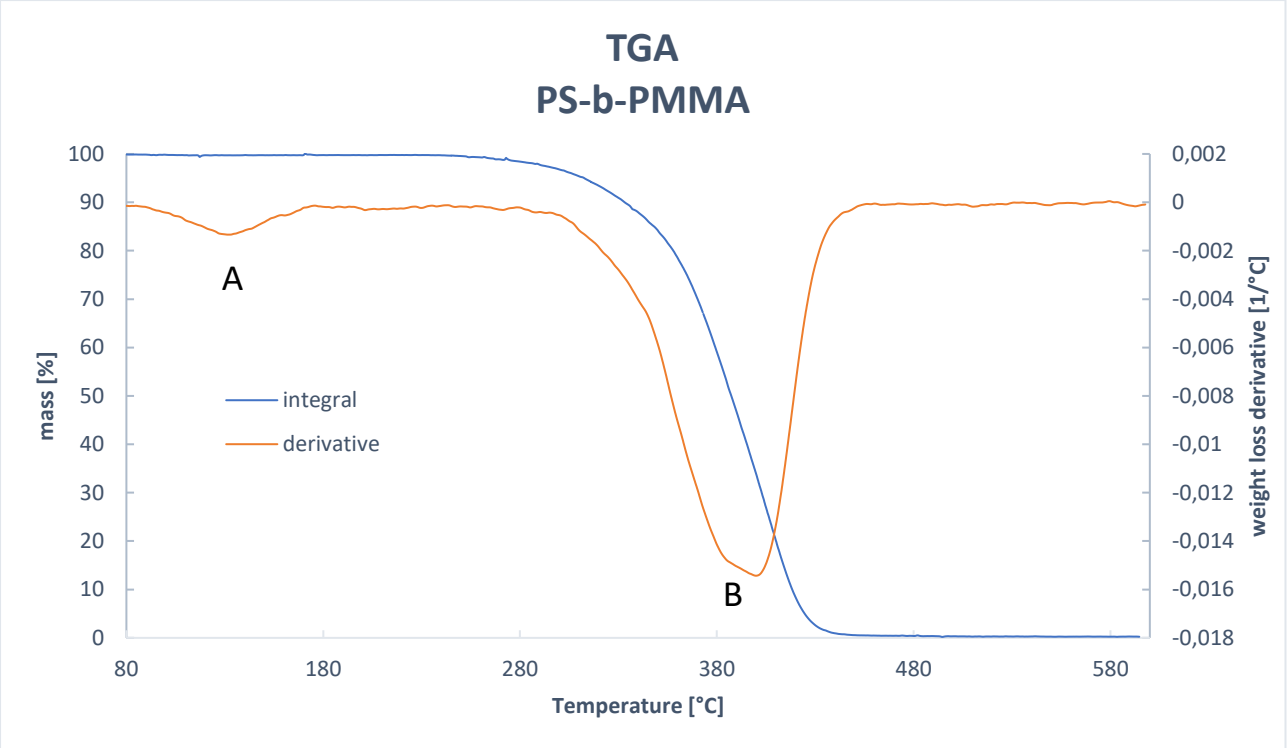

Figura 1.9 TGA PS b PMMA

Per la TGA in figura sono stati utilizzati 0.6740 mg di polimero. Come si può notare dalla curva derivata in figura pare vi siano due step di degradazione per questo copolimero. Analizzando meglio gli intervalli di temperatura in cui si presentano tuttavia, risulta plausibile che il primo picco (identificato con la lettera A) sia attribuibile all'evaporazione di ev. umidità presente nel campione. Questa ipotesi è confermata dalla variazione quasi nulla che si evince dalla curva integrale. Si può dunque affermare che la degradazione termica del polimero dovuta alla decomposizione dei legami della catena principale, la quale avviene in un unico step, ha inizio intorno ai 330°C e raggiunge la velocità massima intorno ai 400°C (punto B della curva derivata). Con questi dati risulta possibile estrapolare la resistenza termica, che può essere fissata a 380°C.

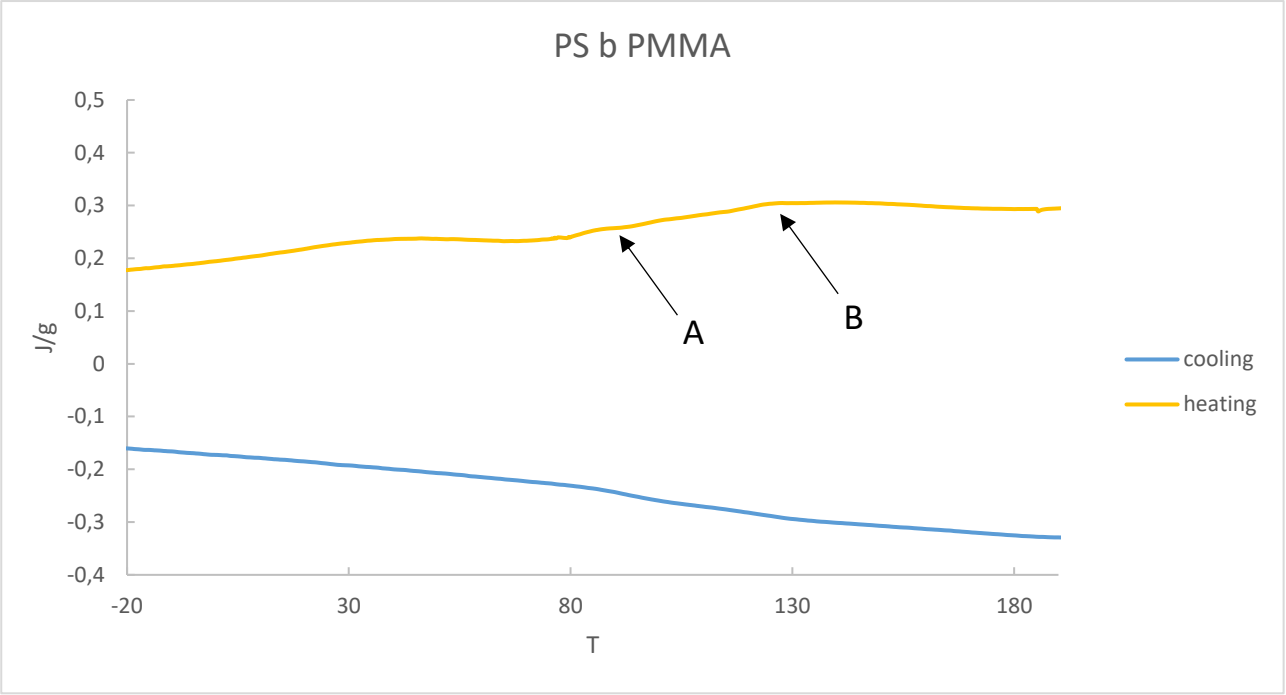

Figura 1.10. Termogrammi DSC per PS b PMMA

Per l'analisi DSC sono stati usati 2.34 mg di polvere. Analizzando la figura è possibile affermare che, come per il PS b P4VP, anche il PS b PMMA è un polimero amorfo; presenta due T_g a 96°C e 128°C (punti A e B in figura). In accordo con quanto trovato nella letteratura, queste temperature risultano prossime alle T_g dei due blocchi che formano il copolimero (100° C per il PS e 130° C per il PMMA). Ciò indica, come per il caso precedente, che a livello microscopico essi risultano appartenere a due fasi differenti.

PS b PCL

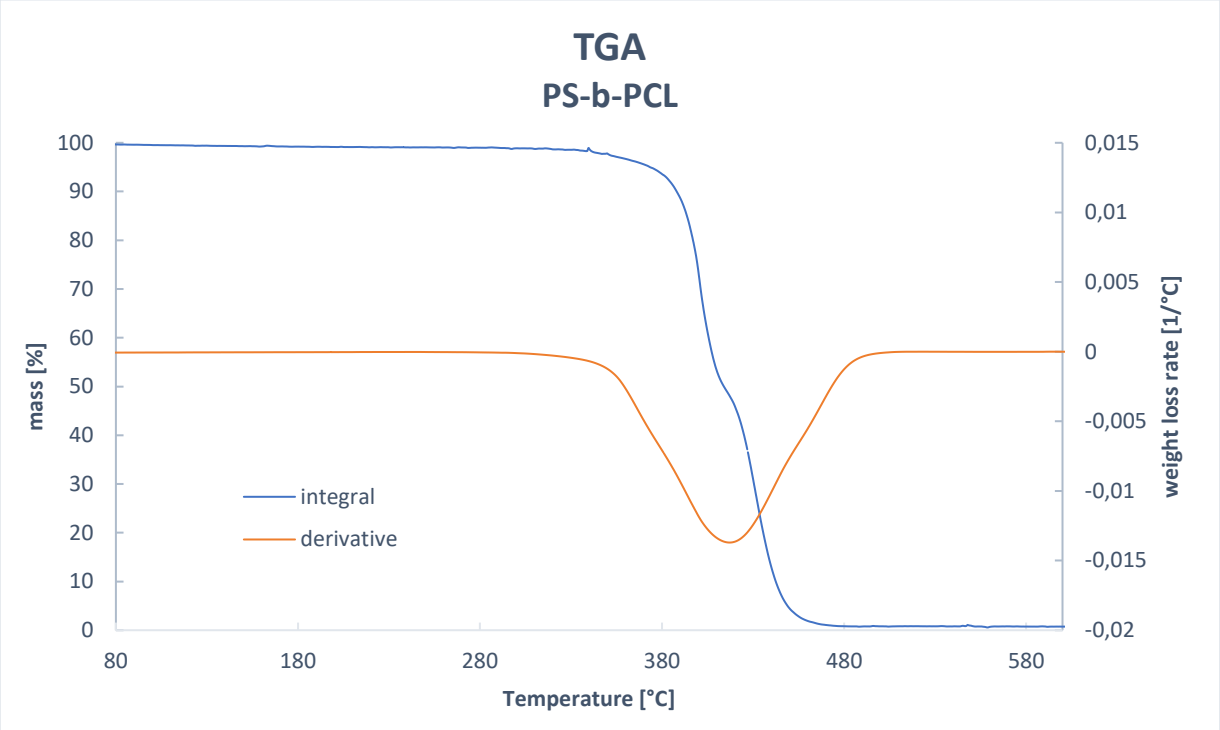

Figura 1.11. TGA PS b PCL

per la TGA di questo polimero sono stati utilizzati 5.2801 mg di polimero. Come osservabile in figura, la degradazione del polimero avviene in un singolo step: sebbene intorno ai 400°C sia presente un piccolo flesso nella curva integrale, la curva derivata conferma che la degradazione avviene in un singolo step; il quale inizia intorno ai 380°C e raggiunge il massimo successivamente, poiché presenta un solo picco intorno ai 417°C, temperatura alla quale la velocità di degradazione risulta massima.

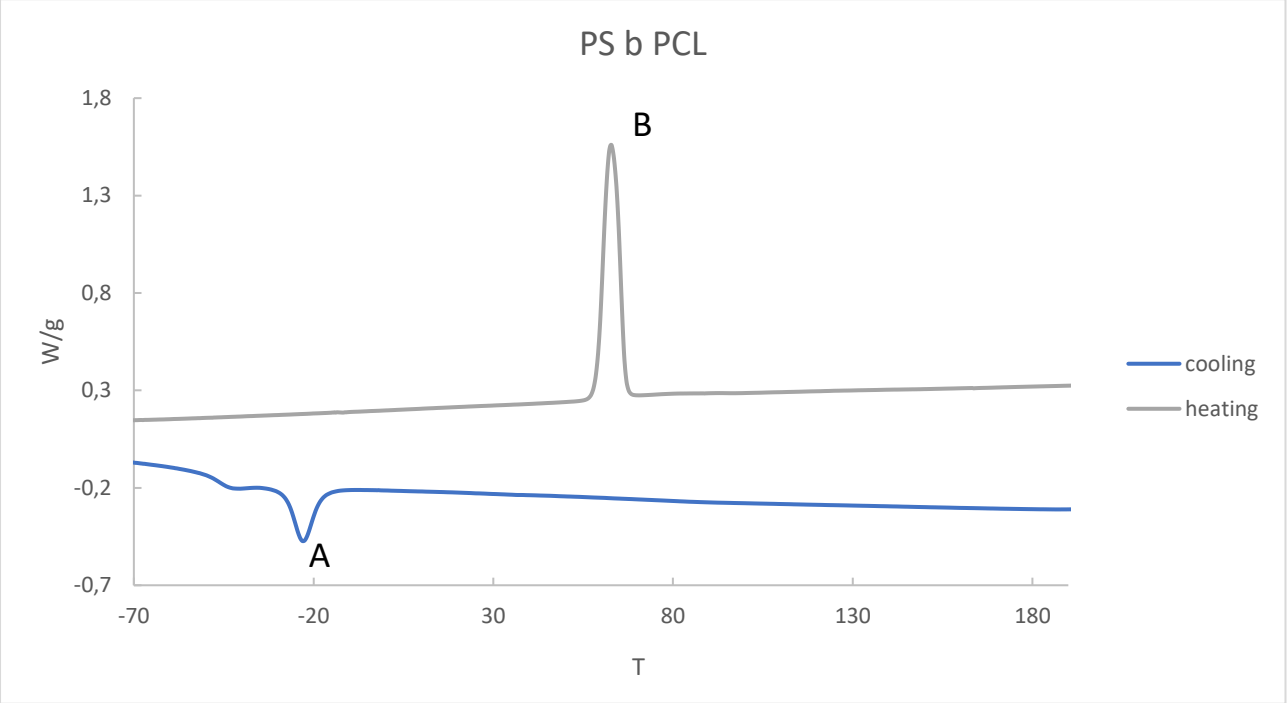

Figura 1.12. Termogrammi DSC per PS b PCL

Per la DSC in questo caso il campione è stato preso di 4.81 mg. Dall'analisi effettuata si nota la presenza di due picchi, dovuti alla presenza di una fase cristallina: il primo picco (A in figura) è dovuto alla cristallizzazione di una fase (che avviene intorno ai - 23°C), ben riconoscibile poiché possiede un valore negativo, mentre l'altro (picco B) denota la presenza di una transizione di fase del primo ordine come la fusione intorno ai 63°C. in accordo con quanto trovato nella letteratura, si è attribuita la presenza di questi picchi alla fasi cristallina del PCL (5% di cristallinità), il quale rappresenta il 30% del copolimero. Un ulteriore approfondimento a tal riguardo verrà compiuto più avanti, durante l'analisi per immagini.

	TDT	Tg	Tm	Tc
PS-b-P4VP	330	104		
	460	149		
PS-b-PMMA	380	96		
		128		
PS-b-PCL	380			-23
			63	

Tabella 1.2. Temperature notevoli ricavate dalle analisi termiche per i vari copolimeri

AFM

PS b P4VP

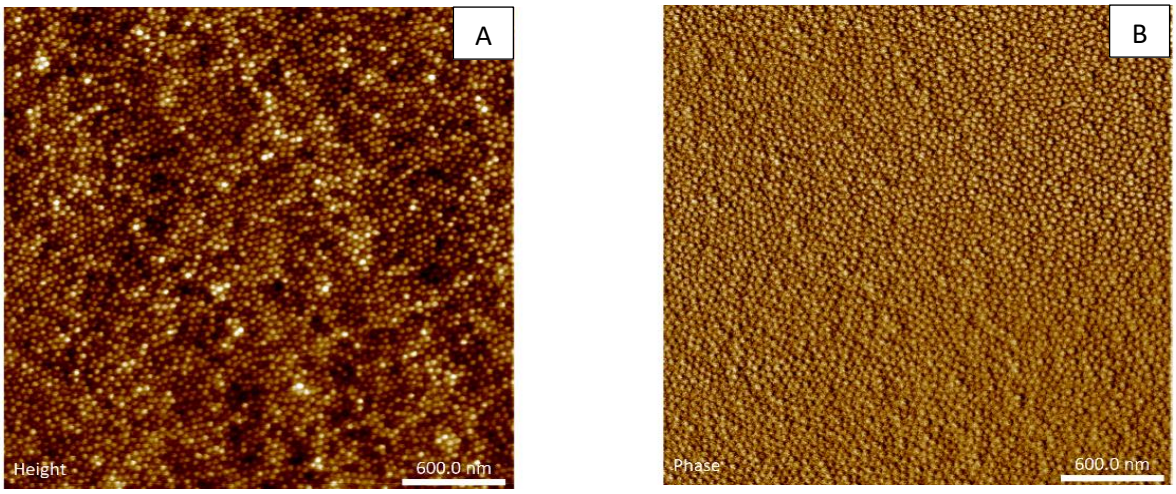

Figura 1.13. Immagini AFM altezza (A) e in fase di PS b P4VP dopo SVA 24h

Dalle immagini in figura è possibile distinguere una morfologia HPC, nella quale i cilindri risultano perpendicolari alla superficie. Soprattutto nell'immagine b, è possibile evidenziare l'apparizione di alcune strisce, le quali possono dare indizi riguardo l'evoluzione morfologica della struttura, per tempi di esposizione maggiori.

Per maggiori tempi di esposizione ai vapori di diossano (il quale risulta un solvente selettivo per il blocco di PS), si ottiene una morfologia di tipo lamellare, come mostrata in figura. La presenza di tale morfologia può essere riconducibile alla maggiore affinità dei domini di PS con l'atmosfera, per cui le macromolecole tendono a migrare verso la superficie. Tuttavia, il processo di diffusione richiede tempo; ciò sembra spiegare la presenza di una morfologia "intermedia" come risulta essere quella HPC, presente solo per periodi di invecchiamento ridotti. In entrambi i casi i domini risultano orientati perpendicolarmente alla superficie, il che denota una certa

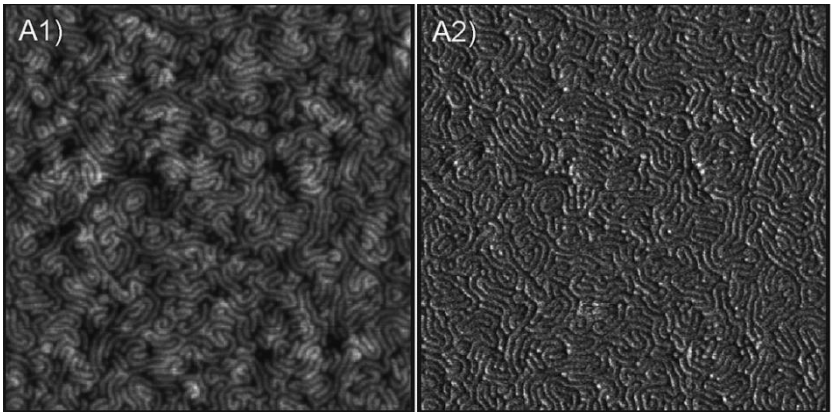

Figura 1.14. Immagini AFM altezza (A1) e in fase (A2) di PS b P4VP dopo SVA 48h

affinità da parte di entrambi i blocchi per l'atmosfera utilizzata. Per questo motivo inoltre, anche il substrato sembra essere neutro per entrambi i blocchi.

PS b PMMA

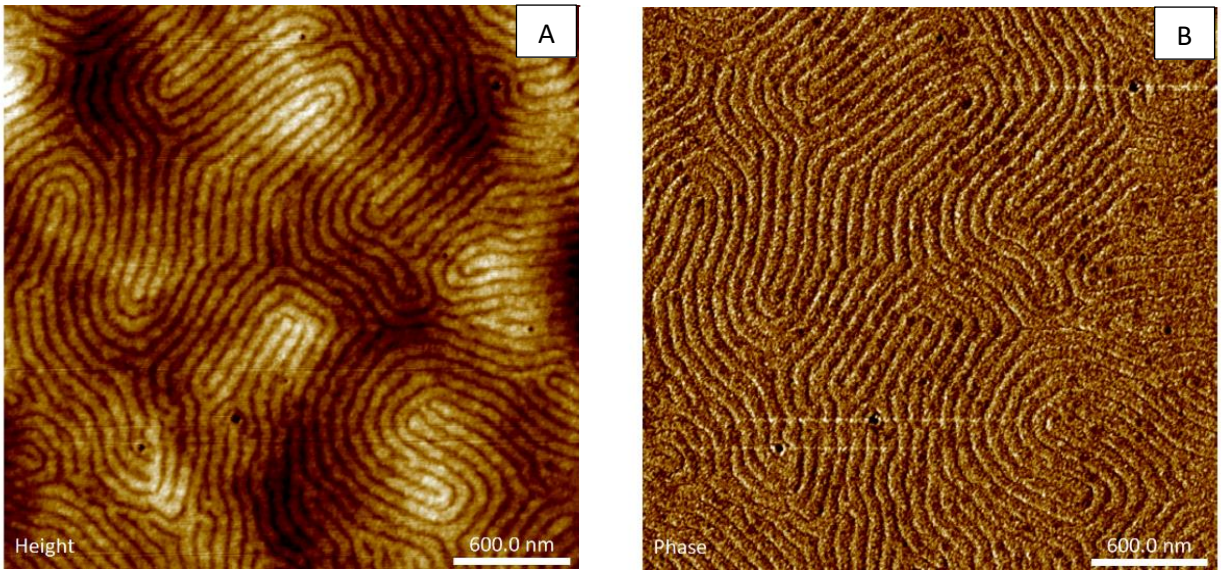

Figura 1.15. Immagini AFM altezza (A) e in fase (B) di PS b PMMA dopo SVA 24h

Da entrambe le immagini una morfologia lamellare ben ordinata e stabile risulta già osservabile dopo sole 24 ore di esposizione; nella quale la distanza media tra una lamella e l'altra risulta essere di circa 77nm. In questo caso le lamelle di PS e PMMA risultano essere spesse 68 nm e 8 nm rispettivamente. Come risulta ben evidente dall'immagine A in figura (nella quale sono ben distinguibili zone più chiare e più scure) la superficie del film possiede una superficie dallo spessore piuttosto irregolare a seconda delle regioni sondate dallo strumento. Nell'immagine in figura B la morfologia lamellare è perfettamente visibile, nella quale le lamelle di colore più chiaro risultano essere di PMMA, mentre quelle più scure risultano appartenere ai blocchi di PS: questa caratteristica è dovuta alla differenza del modulo elastico dei due blocchi (tipicamente 3.0 GPa per il PS contro 3.3 GPa del PMMA), la quale influisce sulla risposta ricevuta dallo strumento in tapping mode. Dopo lo spin coating i blocchi di PMMA sembrano essere situati all'interfaccia con il substrato, mentre quelli di PS risultano in superficie. Durante il processo di invecchiamento il PMMA (il quale possiede maggior affinità con l'acetone) subisce maggiormente lo swelling, per cui comincia a migrare verso la superficie dando origine a questo tipo di struttura.

PS b PCL

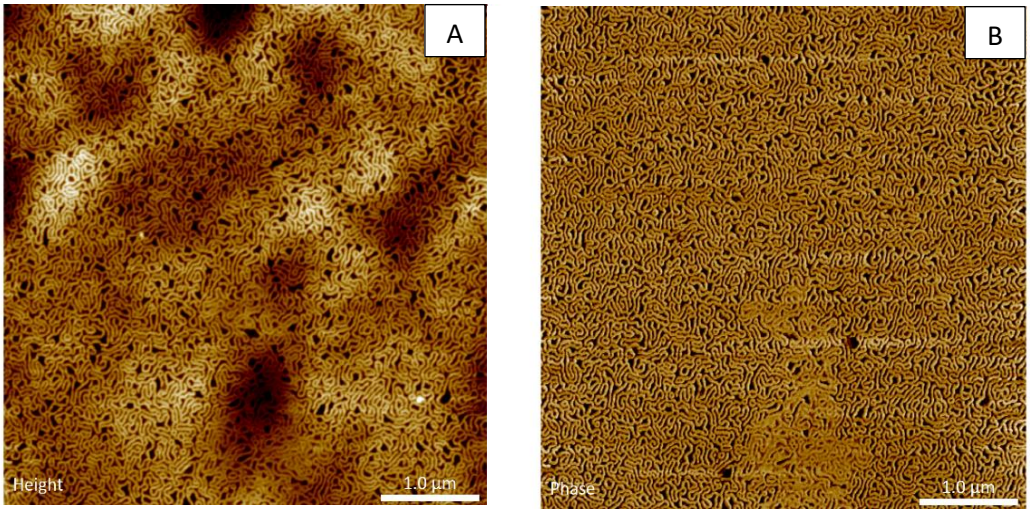

Figura 1.16. Immagini AFM altezza (A) e in fase (B) di PS b PCL dopo thermal annealing a 100°C

Dopo aver sottoposto il film a trattamento termico a 100°C è stata ottenuta una morfologia vermicellare, nella quale i blocchi di PS rappresentano i domini più chiari, poiché sono la fase più dura. Ciononostante, questa struttura non può essere definita ordinata.

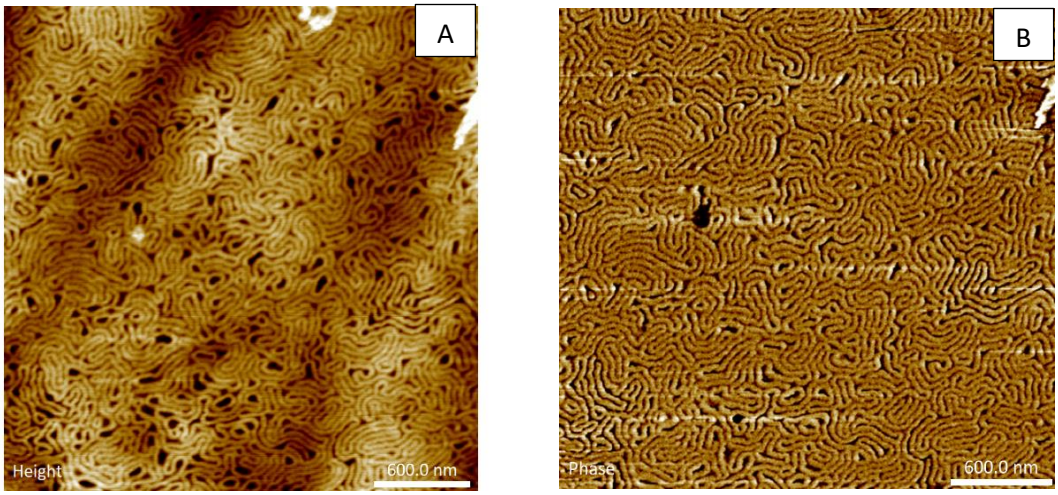

Figura 1.17. Immagini AFM altezza (A) e in fase (B) di PS b PCL dopo thermal annealing a 120°C

Per temperature di invecchiamento più elevate (più lontane quindi dalle T_g) di entrambi i blocchi) le catene possiedono maggior mobilità; riescono quindi a raggiungere una struttura lamellare ben ordinata, in cui le lamelle risultano normali alla superficie.

Vale la pena accennare che, in entrambi i casi, non si notano regioni cristalline per i domini di PCL, come sembrava indicare l'analisi DSC. Ciò è riconducibile alla

percentuale di cristallinità del PCL che risulta ridotta (circa il 5%), mentre la percentuale in peso del PCL nel copolimero risulta essere del 30%; dunque queste fasi non risultano visibili nell'analisi per immagini.

Conclusioni

In questo lavoro, film sottili di copolimeri a due blocchi sono stati caratterizzati dal punto di vista morfologico e termico. Grazie alla struttura controllabile, questi film risultano essere interessanti in diverse e svariate applicazioni di notevole rilievo, dalla medicina alla produzione di dispositivi elettronici sempre più piccoli. Al fine di capire come poter ottenere la struttura desiderata, la caratterizzazione diventa di fondamentale importanza.

Come dimostrato dai risultati ottenuti, i BCP presentano proprietà termiche molto simili a quelle degli omopolimeri corrispondenti ai singoli blocchi. Ciò è ben dimostrato dai valori delle T_g e delle *TDT*, le quali risultano appunto molto simili a quelle dei polimeri costituenti i blocchi.

Come visto attraverso la TGA la combinazione di due diversi polimeri non va ad implementare la resistenza termica del film.

L'analisi dei risultati ottenuti quindi evidenzia che le proprietà più importanti per questo tipo di materiali derivano dalla loro struttura, la quale risulta ordinata a livello nanometrico.

Dall'analisi all'AFM si nota l'importanza dei processi di annealing e, nel caso del thermal annealing, la *TDT* risulta fondamentale per settarne l'intervallo di temperatura stesso. In questo senso, una miglior conoscenza del comportamento in temperatura del materiale permette un'ottimizzazione del processo, quindi un miglior controllo dell'autoassemblaggio. D'altra parte, la comprensione delle interazioni chimiche e di interfaccia tra i differenti elementi in esame (blocchi, atmosfera e substrato) gioca un ruolo fondamentale nel processo di transizione disordine ordine, soprattutto nel caso in cui si ricorra al SVA.

Come provato dai risultati ottenuti tramite AFM, materiali nanostrutturati possono essere ottenuti abbastanza facilmente; con precisione che arriva alla decina di nm. Al contrario di quanto accadrebbe con le lavorazioni meccaniche, in questo caso riusciamo ad ottenere elevatissimi gradi di precisione senza incorrere in perdite di materiale o scarti. Con diverse combinazioni dei parametri di processo è possibile ottenere diverse strutture; tale versatilità è stata provata in questo lavoro per diversi copolimeri.

In questo senso, questo studio va considerato come un punto di partenza per ulteriore e più approfondita ricerca, le quali potrebbe portare a risultati sorprendenti.

2 INTRODUCTION

2.1 BLOCK COPOLYMERS

Block copolymers (BCP) are macromolecules composed by chemically distinct chain segments of different monomers that may be thermodynamically incompatible. The incompatibility of the system leads to segregation (micro or nano-phase separation) of different blocks in domains whose dimensions are in the order of micrometers or nanometers (typically 5-100 nm), giving rise to a wide range of nanostructured materials [1]. Thanks to their many potential applications, a huge amount of studies have been carried out in the last decades and many predictive theories that can account for domain shapes, dimensions, connectivity and ordered symmetry of different types of block copolymers have been formulated [1, 2].

Combining different blocks makes possible to obtain structured materials with tailored mechanical, electrical, barrier and other physical properties. Thanks to different chemical routes a lot of different copolymers can be synthesized. The most common technique to attach different groups of monomers together is the living polymerization of anionically reactive polymers, which permits to obtain the desired structure [3]. The number of possible configurations is quite high, and it is based on the combination of two main parameters: the number of chemically different blocks and their sequence. Taking into account the number of blocks, the most common copolymers are diblock (AB) or triblock (ABC or ABA) ones; whilst their respective structures may spread from the simpler linear ones to the most branched and complex star and hetero-arm ones [4]. Due to the incredible structural and compositional versatility of BCPs, many innovative synthetic strategies have been investigated, generating a previously unattainable architectural complexity of new geometries [1-5].

In this study only diblock copolymers are used to form thin films, so just this class of copolymers will be deepened, despite the topic is actually wider. The simplest and most studied are linear diblock copolymers, in which two different polymer chains are covalently bonded together, forming a new macromolecule [1]. The two segments may be thermodynamically incompatible (immiscible) due to their different chemical structure and composition. If this happens, under certain conditions that will be further explained, they tend to separate (micro or nano-phase segregation); but, as they are covalently bonded, macrophase separation may not occur, leading to a homogeneous material on the macro scale. In this way, they tend to self-assembly into different ordered phases called domains (two in the case of diblock copolymers), constituting the extraordinary feature of these materials.

2.2 BLOCK COPOLYMERS IN BULK

The self-assembly mechanism is driven by the variation of different parameters: the volume fraction of each block ***f***, the Flory-Huggins interaction parameter ***χ*** and the degree of polymerization ***N*** of the copolymer. Although *f* has not a thermodynamic meaning, the Flory-Huggins interaction parameter describes the free energy cost of the contact between dissimilar monomers (Flory 1953), it contains an important enthalpic contribution and it is indirectly proportional to temperature; while *N* reflects both configurational and translational entropy. For this reason, it is commonly used to couple the thermodynamic terms into a product; which results indirectly proportional to the temperature of the system [3, 4, 6, 7]. These parameters influence the behaviour of phase separation, and can be achieved by applying different theories, as the Helfand and co-workers SCF (self-consistent field) theory, which can define free energies, composition profiles and chain conformations [3, 8, 9].

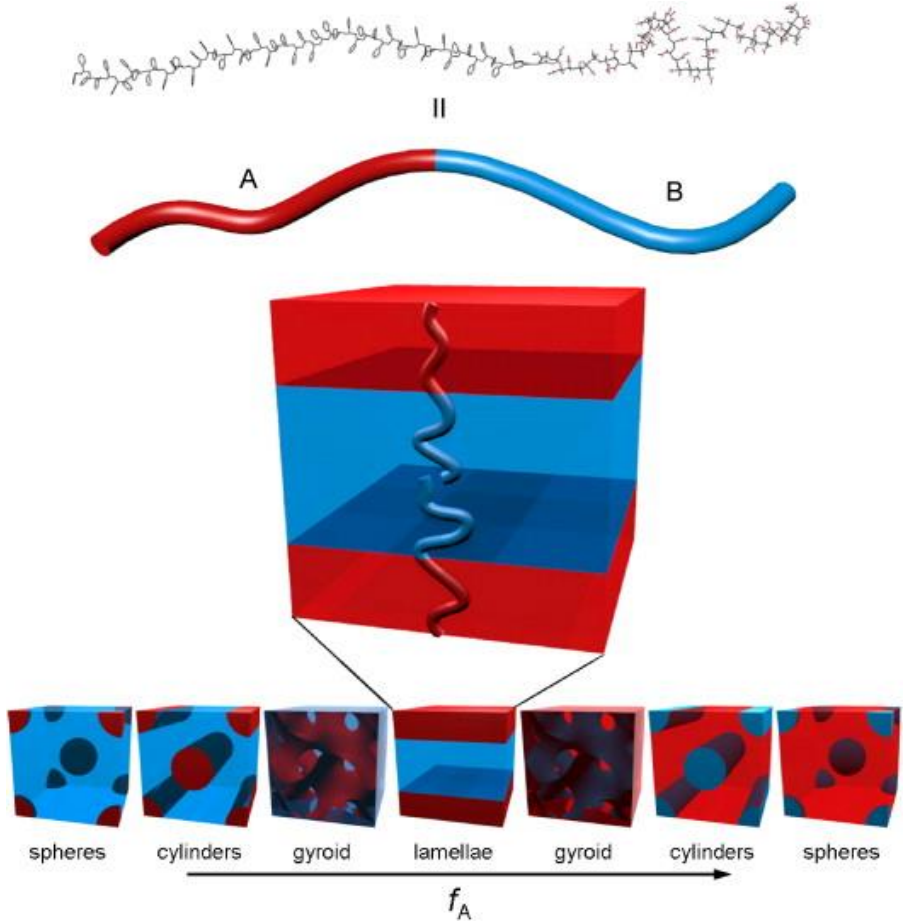

Figure 1. Schematics of thermodynamically stable diblock copolymer phases. The A–B diblock copolymer, such as the PS-b-PMMA molecule represented at the top, is depicted as a simple two-color chain for simplicity. The chains self-organize such that contact between the immiscible blocks is minimized, with the structure determined primarily by the relative lengths of the two polymer blocks (f_A). Reproduced with permission of [7]. Copyright 2019, Elsevier.

As shown in Figure 1, the structure of a diblock copolymer can evolve either changing the χN product or the volume fraction of a block. Thanks to the SCF theory, diagrams like that shown in Figure 2 can be developed, allowing a better understanding of the evolution of phase separation [10, 11].

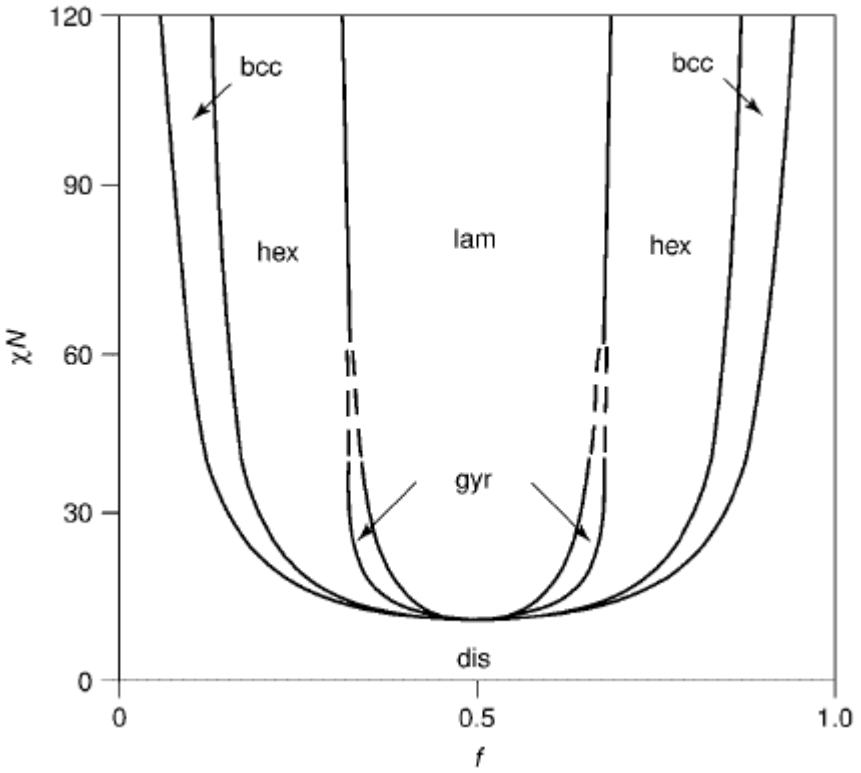

Figure 2. Phase diagram for a conformationally symmetric diblock copolymer, calculated using SCF theory. In the phase diagram, regions of stability of disordered (dis), lamellar (lam), gyroid (gyr), hexagonal (hex), and body-centered cubic (bcc) phases are indicated. Reproduced with permission of [3]. Copyright 2002, John Wiley and sons.

As it was previously pointed out, the separation process is influenced by temperature so, above certain temperature, chains are homogeneously mixed, as any polymer melts. By reducing the temperature, segregation begins. For a volume fraction *f,* at a fixed T called *ODT* (order disorder temperature) a critical value of χN is reached and different blocks begin to separate into different periodically ordered domains. The critical value of χN is not only a function of *T* depending also on the composition of the copolymer. According to Hamley, as it can be seen in Figure 2, for a symmetric diblock copolymer with equal segment sizes, the minimum of the product χN corresponds to f =0.5 and SCF predicts a critical value of $(\chi N)_{ODT}$=10.5 [6]. In this case for such values a lamellar geometry is obtained and, at least teorethically, other geometries can be obtained just by varying either volume fraction or temperature.

Different morphologies for bulk BCPs are commonly obtained by slow cooling the corresponding melts, so that different blocks have enough time to align in the

thermodynamically preferred structures. In this sense, Kim et al. [12] confirmed that there are several analogies between the assembling structure and its thermal history [12]. Reducing the temperature under its glass transition (T_g) in a polymer means trapping the chains in a defined configuration. For this reason, in order to obtain more ordered structures, an annealing treatment (thermal or solvent) is usually done for increasing chain mobility [2], as will be further explained.

2.3 BLOCK COPOLYMERS THIN FILMS

As thin films are obtained by spin coating or casting a dilute copolymer solution onto the substrate, it is worth a short deepening on the behaviour of BCPs in solutions, which becomes fundamental for preparing particular structures with many potential applications such as as surfactants or membranes [3].

The behaviour of BCPs in dilute solutions is controlled by the interactions among blocks as well as by their interaction with the solvent, which may be selective or not for different blocks. If the solvent results selective for one block, micellization may occur. The necessary condition for it is the solution concentration to reach a critical value, called critical micelle concentration (CMC). In this case the core of micelle is formed by the unfavoured blocks of polymer, while the corona contains the selectively solvated blocks [3, 6], as it can be seen in Figure 3.

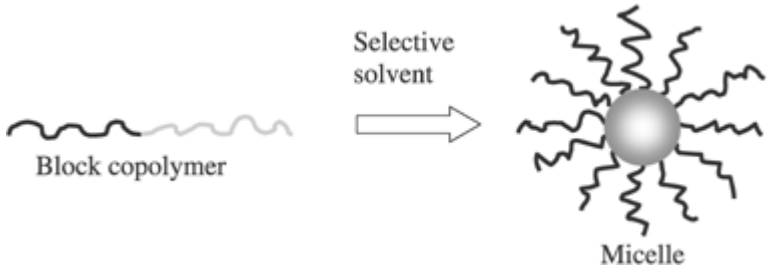

Figure 3. Micelle formation for a linear diblock copolymer. Reproduced with permission of [13]. Copyright 1969, Springer Nature.

For higher concentrations, micelles evolve towards ordered structures, giving rise to self-assembled nanostructures, similar to those obtained for bulk BCPs melts. For further increase in polymer concentration aggregation of micelles occurs, forming a tridimensional structure in which the solvent is entrapped, assuming the behaviour and the aspect of a gel [6].

2.4 SELF-ASSEMBLY IN THIN FILMS

As in this work samples have been prepared in form of thin films, it is worth to describe the differences in the assembling pathway with respect to bulk BCPs.

Thin films consist typically in a thin layer of material (usually of the order of nanometres) deposed on a substrate which may be glass, silica, or special

functionalized and coated materials. They may be prepared by different techniques, the most common one being the spin coating one, in which one or more drops of BCP solution are deposed onto the substrate, whose rotation allows either the spreading of the solution by centrifugal forces or the driving off of the volatile solvent. The main advantages of this technique are the ease of control of operational parameters such as the spinning speed and time, which permits to reach a uniform thickness and a limited roughness of the obtained film. For these reasons spin coating is the most used technique, even if other methods like dip coating or direct solvent casting are also reliable [3].

The main difference between bulk BCPs and thin films derives from the presence of an interface not only with atmosphere, but also with the substrate. Another important factor that affects the structure is the thickness t, which results to be comparable with the periodicity of domains L_0. These two facts lead to differences in the self-assembled structures.

In several works [14,15] a general higher degree of order has been observed for thin films with $t<L_0$ respect to bulk BCPs, which are typically characterized by grains of ordered domains randomly oriented to each other [16]. This fact is due not only to the minor thickness (minor "gradient of order") but the result of the interfacial energy minimization which follows this arrangement.

An important aspect that should be analysed is the presence of asymmetric boundary conditions, because the surface energy between each block and its substrate/atmosphere may differ by an order of magnitude. This fact obviously implies a different behaviour of blocks at the two interfaces, which follows the minimization of the energy of the system. In case of thin structures these boundary effects become important for the whole thickness of the material. From this it emerges that surface energy and surface chemistry are the driving forces of the ordering process. The substrate/block forces may be attractive or repulsive, the same for the wettability which may be higher or lower for each block. For these reasons it is possible to divide surfaces into two families: neutral surfaces and preferential surfaces [16]. Preferential surfaces promote the contact with only one block, while neutral surfaces promote the contact with both. In the first case a lamellar geometry is preferred (with just one block in contact with the surface with a parallel orientation) whereas in the other case, any geometry allowing a good contact between the substrate and both blocks will be promoted, resulting into different orientations, as it

can be seen in Figure 4. It has to be remarked that, as in thin films there are always two different surfaces, hybrid morphologies may appear [18].

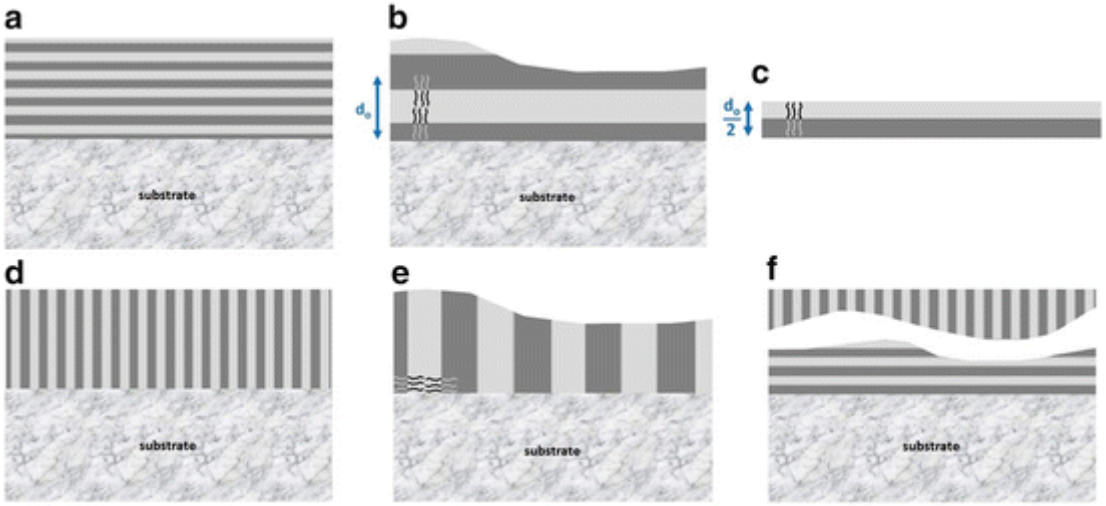

Figure 4. Schematic representation of various alignment situations: (a) and (b) show parallel alignment, (c) represents the elementary brick constituting parallel aligned films, (d) and (e) show perpendicular alignment, (f) shows a mixed alignment. Reproduced with permission of [18]. Copyright 2015, Springer Nature.

BCP thin films show commensurability effects between the film thickness and the morphological repeating structure spacing in the normal direction [19]. This may affect the surface topography of the film, which may become an important aspect to consider either when surface analysis will be carried out (by atomic force microscopy, AFM, like in this work) [5] or for technological applications [20]. The structure is in equilibrium only if the thickness of the film is equal to an integer value of the periodicity parameter L_0, if not residual stresses may rise. If this condition is not reached the residual stresses upon the annealing process lead to the formation of areas of different thickness, commonly called “islands” and “holes”. In such structure (shown in Figure 5) it is possible to distinguish step-like isolated terraces and depressions, which can influence the surface morphological patterning of the film. This phenomenon has been most studied for lamellar structures but has also been seen for other morphologies [16].

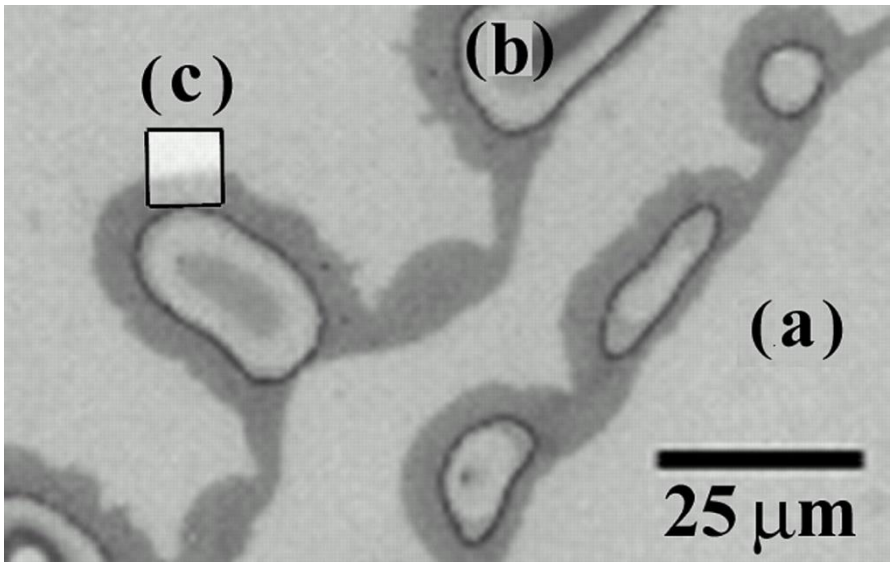

Figure 5. Optical micrograph of lamellar PS-b-PnBMA droplets exhibiting surface parallel lamellae morphology and the terracing phenomenon. (*a*) Silicon substrate, (*b*) terraced droplet. Bands of contrast indicate specific optical interference conditions caused by quantized L_0-sized (43 nm) jumps in film thickness. (*c*) Example area (light box) for AFM analysis. An exposed region of bare substrate allows film thickness determination. Reproduced with permission of [16]. Copyright 2001, Annual Reviews.

Another important effect on the ordered structure of thin films, lies in the morphological aspect of the substrate. It not only plays a role in terms of surface energy, but eventually also the presence of a pattern may influence the order of BCP domains. The first effect is seen in a rough surface; if the roughness characteristic length of the surface is larger than the period of the nanostructure, a perpendicular alignment is always favoured, even for low characteristic roughness height. Instead of the "natural" roughness, a surface pattern could be created by templating it with traditional lithography. In this case dimensions are orders of magnitude higher than the BCP structure parameters but can however induce a particular structure in it. The same results can be achieved by chemically patterning the surface of the substrate.
Another way to influence the self-assembly process of thin films is treating the surface of the substrate by grafting to it a random copolymer with the same chemical composition than the BCP used for the film, tuning the surface energy of the substrate and so inducing the assembly of the preferred structure [18].

2.5 ANNEALING TECHNIQUES

Usually spun films show a quite disordered structure, mainly due to the rapid evaporation of the solvent. The fast evaporation traps polymer chains in a poorly ordered state and, because of the temperature, which in many cases is well below the T_g of each block, they don't have enough mobility to evolve to thermodynamic

equilibrium [21]. For this reason, many treatments are used further spin coating, in order to give enough mobility (either using heat or solvent vapour) to the chains for reaching an ordered structure, obtaining the microphase separation of domains.

2.5.1 Thermal Annealing

The increase of temperature above the T_g of each block gives enough mobility to the chains to allow their reciprocal movement and rearrangement into the equilibrium morphology. The treatment may be performed for long times (usually some days), to allow the structure to reach the ordered structure, typical of the equilibrium state, depending on the copolymer. Main parameters in this treatment are *T* and *t*, together with the environment and pressure. As this last parameter plays an important role, [21], it is common to perform thermal annealing in vacuum, as it can be seen in Figure 6. It has been proven that heating rate doesn't affect the ordering process, while cooling rate is an important parameter, especially because it influences the surface reordering [23]. Unfortunately, as shown in many works as in Ferraresi et al. [24], this technique often requires an annealing time on a scale comprised between 10^2 and 10^3 min, which could be an issue in the industrialization stepforward for instance.

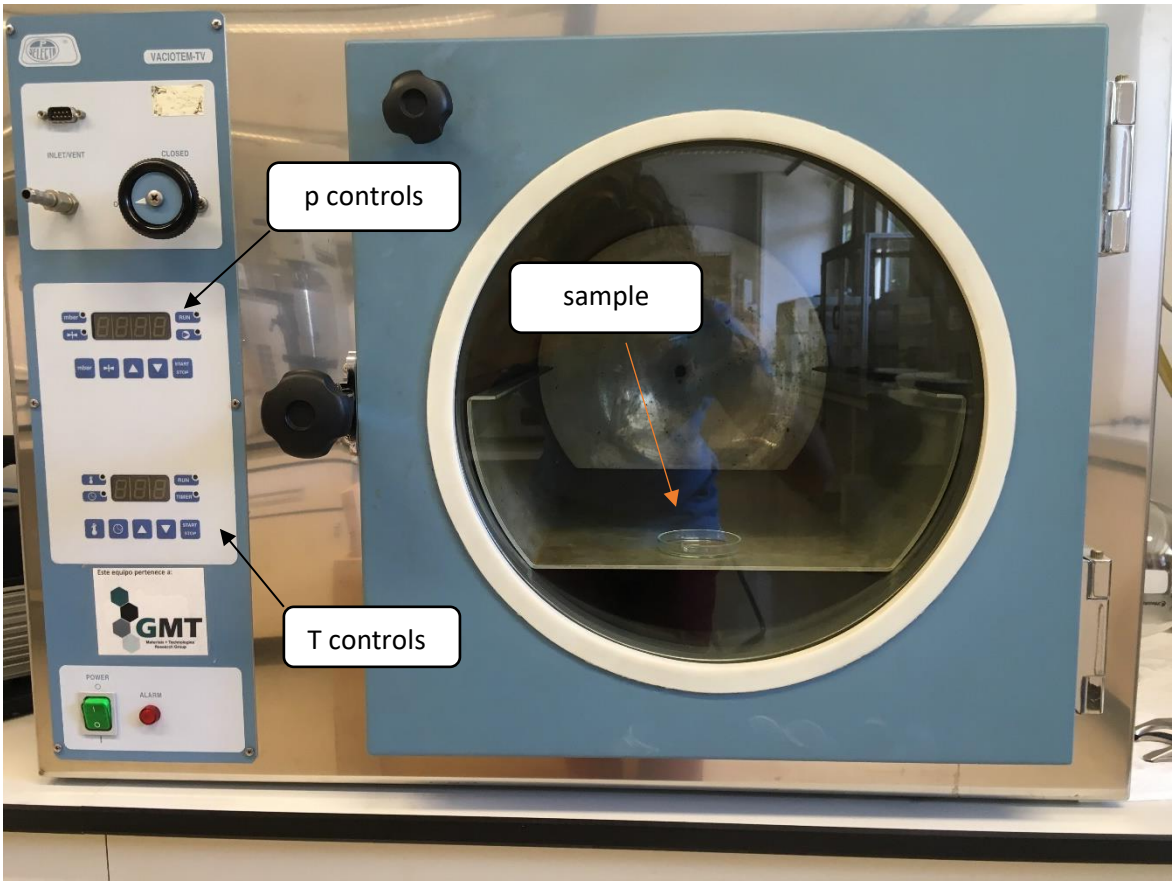

Figure 6. Vacuum oven used for thermal annealing treatments

Another disadvantage of this technique is the temperature of the process: microphase segregation may only appear in a narrow range of temperature, between T_g and thermal degradation temperature, which may require great attention [17, 21-24]. Thanks to the control of annealing temperature different ordered structures, with different periodicities can be obtained, as it is shown in Figure 7.

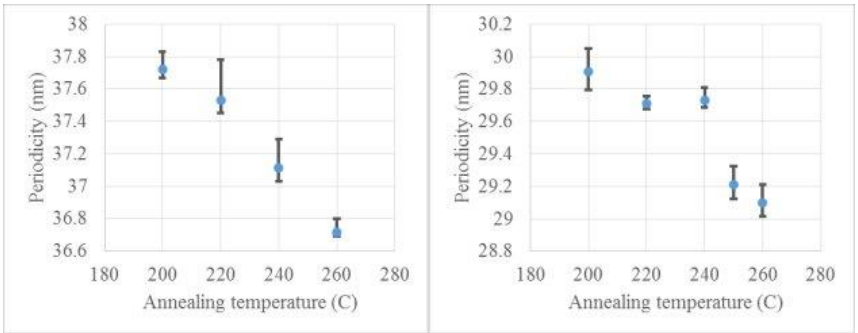

Figure 7. Effect of annealing temperature on the periodicity of domains. Reproduced with permission of [22]. Copyright 2018, Springer Nature.

2.5.2 Solvent Vapour annealing (SVA)

In order to avoid above mentioned issues, exposing the BCP film to the vapours of a specific solvent represents a good option to obtain long range ordered structures. This technique reveals also another advantage, which relies in the possibility of obtaining different structures without the need of any pre-treatment of BCPs or substrates [25].

The process itself consists in exposing the spun film to a solvent vapour for a certain time, or by using a controlled atmosphere or a carrying gas. In the first case, the simplest configuration involves a solvent reservoir enclosed in a “bell jar” together with the polymer film for a certain period [17]. In the other procedure, the solvent reservoir is outside of the annealing chamber and an inert gas is compressed and used to make the solvent bubble, carrying it in its stream. Then it is sent to the annealing chamber where the contact between the vapour and the film occurs. The second solution permits a better control of the partial pressure of the vapour, by adjusting the mixing ratio gas/solvent [21, 22]. Although the first solution is easier to set up and it is widely used in any laboratory, it is less precise, and it does not result ideal to control some important parameters such as partial vapour pressure of solvent or its removal rate after the annealing treatment.

SVA process consist on two different stages: the first one represents the time necessary to reach the swollen state, while the second is represented by the time for solvent evaporation (deswelling/evaporation).

The solvent uptake is affected by the chemical affinity of the solvent with each block, besides their physical state (i.e. glassy, rubbery, semi-crystalline, etc). This means that each block may swell differently, resulting in an effective variation of the volume fraction of blocks, which directly affects the assembling of domains in an ordered structure. The swelling process is favoured by the incompatibility of each block, diluting the interface between them, and continues until the chemical potential of the solvent in the film equals that of the solvent in the vapor phase [25]. The ordering of the whole is not achieved instantaneously but progresses with a front (ordering front) as the solvent vapor diffuse trough the thickness, being the diffusion parameter (diffusivity) which controls the first stage of SVA, the swelling. The thickness of the swollen state is controlled by the vapour pressure, so for the respective polymer/solvent concentration; which directly influences the structure assumed by the swollen state and thus the symmetry of the dry film [26]. From this fact it emerges the crucial role of the partial pressure of the vapour in the annealing chamber, and importance of its control. The structure assumed by the BCP in the process also depends on the time taken for the swelling process. The structure of the swollen films is being well studied, in order to know better the SVA ordering mechanisms which still present some unanswered questions [25]. After this, the next step is the removal of the sample from the vapor environment, and its subsequent evaporation from the film. While evaporating, it leaves an ordered structure behind, whose front proceeds inward respect to the direction of solvent driving off. During this stage of the process a slow uptake of the solvent is suggested, in order to obtain an ordered self-assembled structure. Figure 8 shows a scheme of the solvent evaporation during the process.

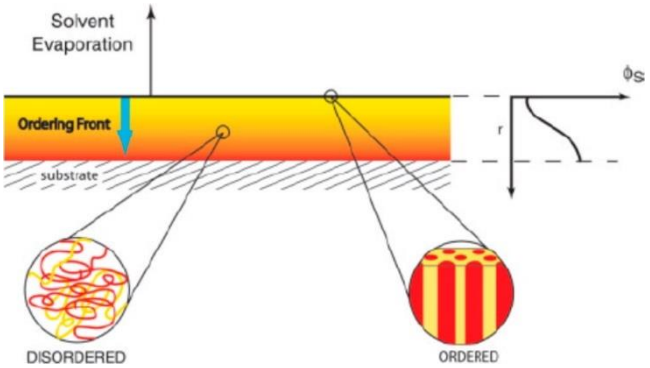

Figure 8. Schematic view of the solvent evaporation in a thin block copolymer film illustrating the concept on an ordering front that propagates through the film inward the evaporation direction. Reproduced with permission of [26]. Copyright 2013, American Chemical Society.

During vapour exposure polymer chains absorb solvent molecules, leading to a swelling of the film. If a neutral solvent is used (it has not better affinity with any of the blocks) it provides enough mobility to the chains to rearrange in a long range ordered structure, reaching the equilibrium morphology [26].

2.6 NANOSTRUCTURED MORPHOLOGIES

At this point, the parameters that govern self- assembling process should be clearer, so it will be easier to understand how and why different structures could be found under different conditions or after certain treatments. Although there is a large research work on this topic, the deep description of morphologies is not the aim of this work, so the reader will find here just an introduction, which should be useful for a better understanding of experimental part shown below.

2.6.1 Lamellar morphology

The simplest stable phase for linear diblock copolymer thin films is the lamellar morphology (LAM). It could be obtained either without any treatment or after annealing (SVA or thermal). In both cases defects are reduced, and so are residual stresses. This step is particularly useful for obtaining more ordered structures. The orientation of lamellae depends on many parameters as annealing time, T and pressure, film preparation; but it also depends on the molecular structure (chain length and molar mass) of the polymer [4, 17].

In the case of thin films, the affinity with the substrate plays a key role in the orientation of domains, as well as the morphology of its surface, while film thickness suffers commensurability effects, which may lead to the presence of the so-called holes and islands [6]. This parameter not only affects surface morphology of the film, but it may also influence the orientation of lamellae [16, 20].

2.6.2 Hexagonally packed cylinders morphology

This morphology is defined as a bunch of perpendicular cylinders packed to form a hexagon (HPC). It is another stable morphology for thin BCPs films, more typical for asymmetric diblock copolymers and for BCPs containing one or more liquid crystal blocks; its presence also depends on the same factors explained for lamellar morphology [4]. According to the literature the morphological transformation from hexagonally packed cylinders to lamellae may be induced either by an annealing treatment or by adding inorganic components such as nanoparticles [27, 28].

2.6.3 Gyroid morphology

Gyroid morphology (G), in contrast with HPC and LAM, can exist just for a narrow composition interval, as widely stated in literature [4, 6, 10, 11] and shown in Figure 2. This kind of morphology may be useful for producing mesoporous or nanoporous

structures, which may present different potential applications. This morphology has been found for different copolymers, as those with a supramolecular structures [4].

2.6.4 Spherical morphology

Spherical morphologies consist in spheres of one block packed in an ordered cubic structure of the other block. This structure may be body centred (BCC) or face centred (FCC). Both morphologies, in contrast with LAM and HPC ones, are isotropic; so the orientation of these structures is not as complicated as for the others [4, 29].

2.7 APPLICATIONS

As BCPs thin films could be interesting for many potential applications, their study has increased during the last decade. One interesting application lies in the production of electronic device like high-density data storage media, in which thanks to their nanoscale structure order, they could find their place as tuneable masks in nanolithography, as it is shown in Figure 10. In this way, two of the largest companies in the market as IBM and HGST have already applied, or are going to, BCP in micro-chips manufacturing [30]. Due to the limits of UV photolithography, nanolithography is gaining interest in the industry of semiconductors. In different works nano-lithographic etching processes have been investigated [31]. In these techniques, using different etching steps, the ordered structure of thin films is transferred to a different

substrate, allowing the patterning of surfaces with a never seen high precision, on nanometric scale [31].

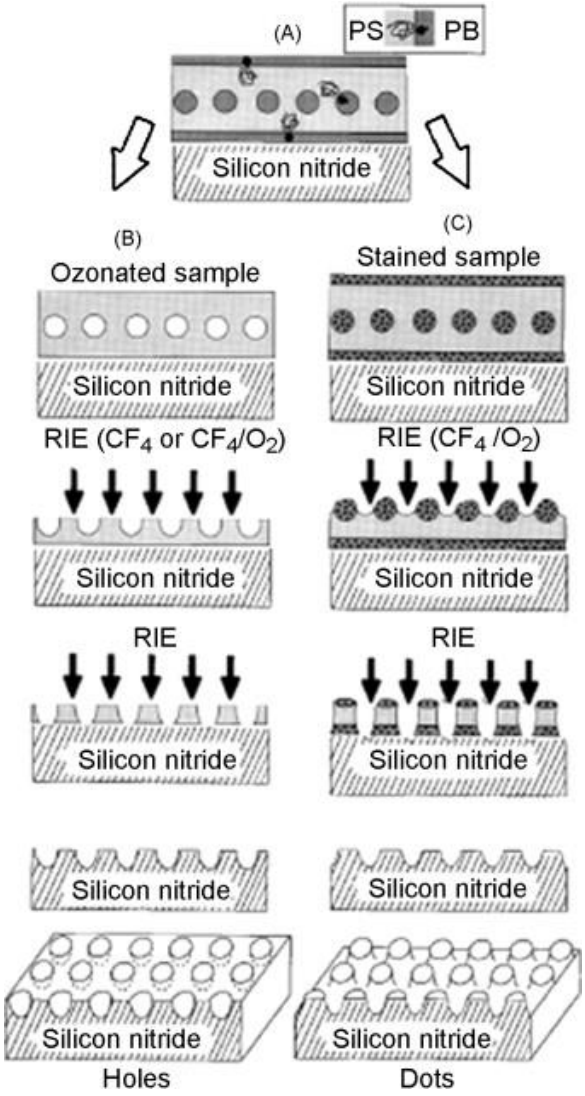

Figure 10. Schematic cross-sectional view of a nanolithography template, consisting of a uniform monolayer of polybutadiene (PB) spherical microdomains in a polystyrene (PS) matrix, supported on silicon nitride; PB wets the air and substrate interfaces. Reproduced with permission of [32]. Copyright 2009, Elsevier.

Another interesting application of BCPs thin films is as templates for inorganic materials, with which mesoporous structures of silica and titania have been obtained. Always through etching processes BCPs films may allow to obtain nanoporous

materials for catalysis applications as nanowires or dots metallic arrays, as it is shown in Figure 11.

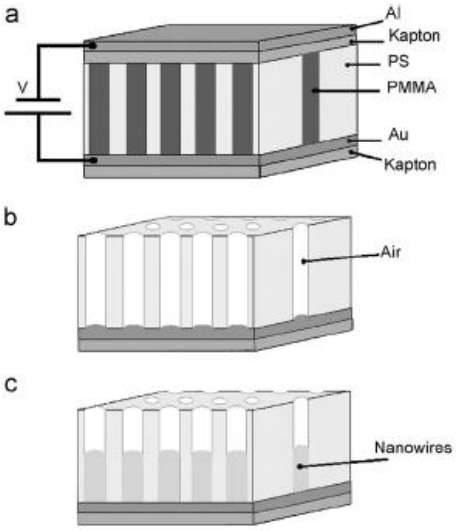

Figure 11. Schematic example of the process for obtaining nanowires from BCPs: (a) An asymmetric diblock copolymer annealed above Tg under an applied electric field, forming a hexagonal array of cylinders oriented normal to the film surface. (b) After the removal of the minor component, a nanoporous film is formed. (c) By electrodeposition, nanowires can be grown in the porous template. Reproduced with permission of [7]. Copyright 2007, Elsevier.

Moreover, these materials find another applications such as membranes for water filtration [32], new generation photovoltaics [4,33], among others.

3 MATERIALS AND METHODS

3.1 BLOCK COPOLYMERS

3.1.1 PS-b-P4VP

PS b P4VP is a linear diblock copolymer composed by a (poly)styrene (PS) block and a (poly)4-vinylpyridine (P4VP) block. PS is a thermoplastic hydrophobic polymer widely used for many applications, while poly 4-vinylpyridine (P4VP) contains nitrogen atoms, which make the molecule hydrophilic. Chemical structures of both monomers can be seen in Figure 12.

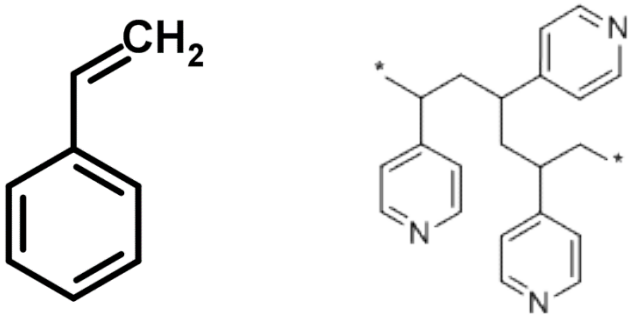

Figure 12. Chemical structures of styrene and 4-vynilpyridine monomers [34,35]

Poly(styrene-b-4vinylpyridine) block copolymer was purchased from Polymer Source with average molecular weight (M_n) of 22500 and 29000 g/mol for PS and P4VP blocks respectively, and a polydispersity index (M_w/M_n) of 1.2 for both blocks.

3.1.2 PS-b-PMMA

Poly(styrene-b-methylmetharcylate) (PS-b-PMMA) is a linear diblock copolymer, containing PS and polymethylmethacrylate (PMMA) blocks. PMMA is a vinylic thermoplastic polymer, widely used to substitute glass in many applications. Chemical structure of the monomer can be seen in Figure 13.

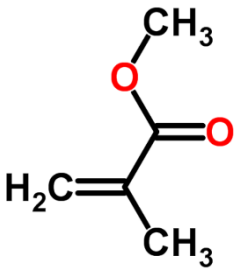

Figure 13. Methylmethacrylate monomer [34]

PS-b-PMMA block copolymer was purchased from Polymer Source, with an average molecular weight (M_n) of 80000 and polydispersity index (M_w/M_n) of 1.09 for both blocks.

3.1.3 PS-b-PCL

Poly(styrene-b-caprolactone) (PS-b-PCL) is a diblock linear copolymer, with PS and the more hydrophilic PCL block. Polycaprolactone (PCL) is a biodegradable polyester widely used in bio medics. It is highly hydrophilic, thanks to the presence of the oxygen [36]. The monomeric structure can be seen in Figure 14.

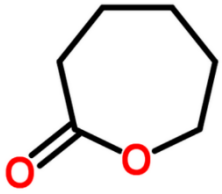

Figure 14. Caprolactone monomer [34]

PS b PCL was purchased from polymer source, with an average molecular weight (M_n) of 27000 and 10000 g/mol for PS and PCL blocks respectively; while the polydispersity index is 1.25 for both.

3.2 FILMS PREPARATION

According to the literature, the spin coating technique has been chosen for sample preparation. Firstly, it is necessary to prepare a solution of each polymer. In order to choose a proper solvent, it is fundamental the knowledge of the solubility: the affinity of a polymer and a solvent depends strongly on the Flory-Huggins parameter χ, which may be obtained from the solubility parameters of the components, as shown in equation 1.

$$\chi \approx 0.34 + \frac{V}{RT}\left(\delta_p - \delta_s\right)^2$$

While the solubility is expressed by equation 2 as:

$$\delta = \sqrt{\frac{\Delta H_v - RT}{V}}$$

Where δ is the solubility (of polymer and solvent respectively), V is the solvent specific volume, T the temperature, R the ideal gases constant and ΔH_v the enthalpy of vaporization. This parameter is a measure of intermolecular forces in the solution.

According to the literature a polymer may be considered soluble in a solvent if $\chi \leq 0.5$ [37-40]. Solubility parameters of all blocks used in the present work can be seen in Table 1.

	H_2O	EtOH	TOLUENE	ACETONE	DMF	DIOXANE	THF
χ_{PS}	4,817	0,377	0,684	0,157	0,212	0,100	0,448
χ_{P4VP}	4,522	0,241	0,985	0,285	0,102	0,216	0,662
χ_{PMMA}	6,091	1,222	0,027	0,024	1,056	0,078	0,008
χ_{PCL}	6,007	1,155	0,043	0,015	0,984	0,058	0,016

Table 1. Some χ values for blocks and solvents used in this work, compared with solvents currently used in daily life (water and ethanol) too. The calculations have been made at 25°C and data come from [40-42]

Taking this into account, the solutions of different copolymers were prepared as it follows.

3.2.1 Solutions Preparation

3.2.1.1 PS b P4VP

The preparation started weighting an amount of 0.084g of PS-b-P4VP powder and solved into the necessary amount of solvent for obtaining a 1% (weight) solution. For the preparation of this sample, DMF was chosen as solvent, which, according to literature and Table 1, may be considered a poor solvent for PS block and a good solvent for P4VP one. For promoting the solubilization process magnetic stirring was used, as shown in Figure 15. The resulting transparent solution will be called solution 1.

Figure 15. Magnetic stirring set up for preparing copolymer solutions

3.2.1.2 PS-b-PMMA films

At first 0.097 g of polymeric powder have been dissolved in 10.790 ml of THF with the help of magnetic stirring, obtaining a clear transparent solution at 1% (weight). The so obtained solution will be called solution 2. In this case THF results a good solvent for PMMA but a poor one for PS.

3.2.1.3 PS-b-PCL films

The starting amount of polymer was 0.088 g, to which 10.063 ml of toluene (TOL) were added, obtaining a clear, transparent, 1% (weight) solution (solution 3). Also in this case, the solvent preferentially dissolves PCL blocks instead of PS ones.

3.2.2 Substrate Preparation

For the preparation of this group of samples a glass substrate with no further treatment was used. Using a diamond-tip tool, squares of around 1 cm length were cut, and cleaned using ethanol.

3.2.3 Spin Coating Process

As said above, spin coating technique was chosen to prepare the series of samples used for AFM analysis. According to the literature this technique permits to obtain films with homogeneous thickness and a reduced roughness, which is important to obtain good quality AFM images [3,6]. For solution 1 six samples were prepared: three with one drop of solution and three with two drops. For solution 2 two samples made by one drop each one were prepared. For solution 3 six samples of one drop were prepared. All the samples were put in the spin coater (P6700 series by specialty

coating systems), shown in Figure 16, and they were treated with the P3 program (120 s @2000 rpm).

Figure 16. The spin coating set up used in this work

As it is shown in Figure 17, thin transparent films were obtained.

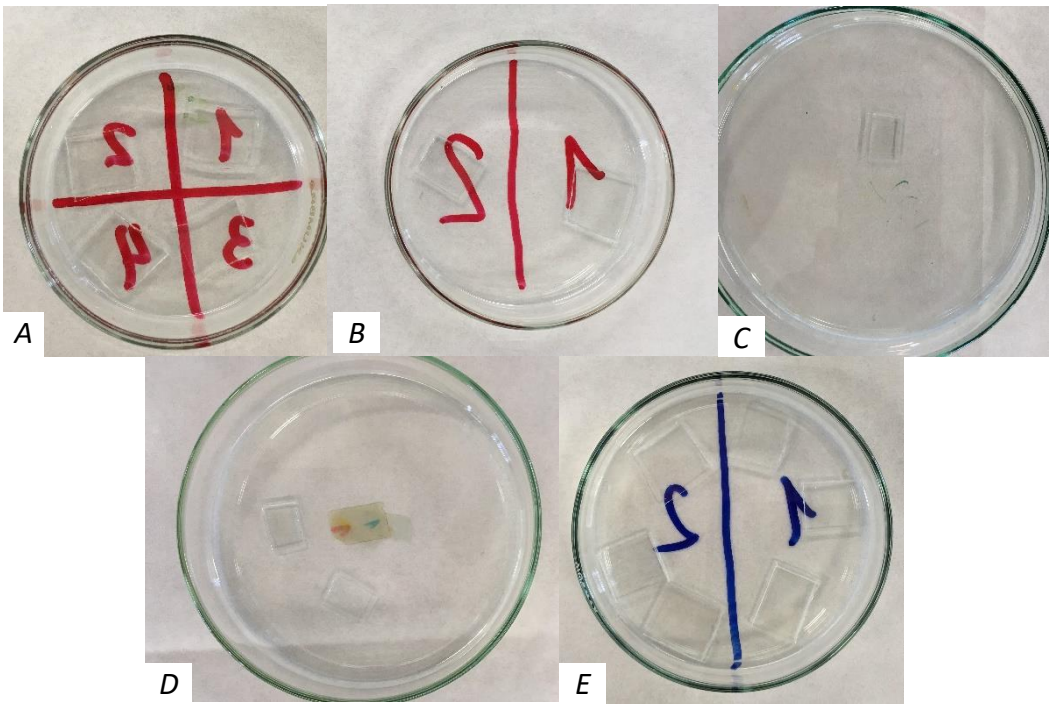

Figure 17. A, B) PS-b-P4VP samples (1,3 in A and 1 in B with two drops, 2,4 in A and 2 in B with one drop); C,D) PS-b-PMMA samples; E) PS-b-PCL samples (either 1 and 2 with one drop of solution)

Each group of samples will be treated with a different annealing process, as it will be shown below. Nevertheless the number of samples, just one image for each type will be taken (the most clear).

3.2.4 Annealing treatments

As mentioned in the introduction chapter, in order to obtain highly ordered morphologies an annealing process is strongly suggested. In this work either thermal or solvent vapour annealing were performed, evaluating the effects of process parameters, such as T and time. For PS-b-P4VP and PS-b-PMMA solvent vapour annealing was performed, varying the exposure time for each sample from 24h to 48h. The set up for this process is shown in Figure 18.

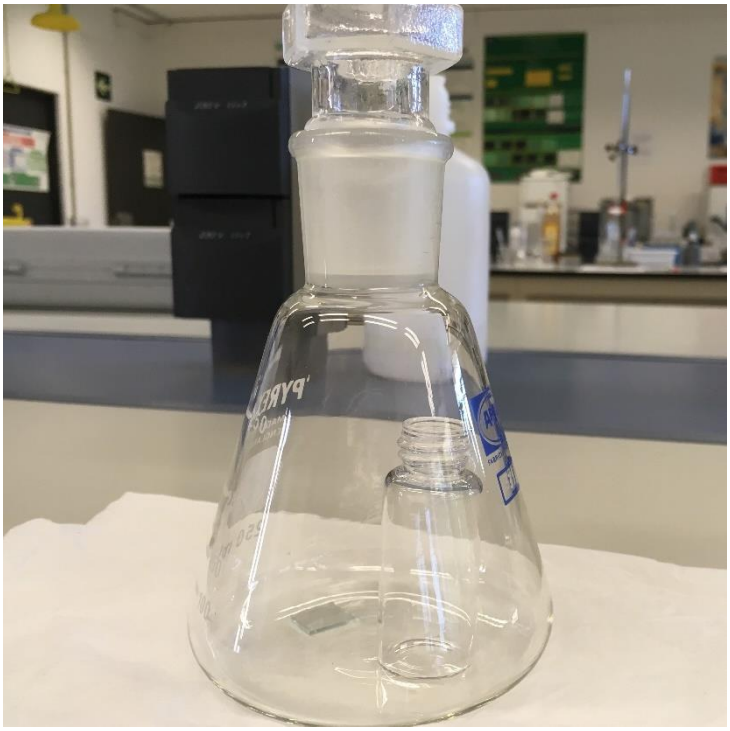

Figure 18. Experimental set up for SVA process

As it is shown in the figure, the film was placed in a capped conical flask, together with a 12 ml cylindrical container filled with 9 ml of solvent. For PS-b-P4VP dioxane was used, which is a selective solvent for the PS block; whilst for PS-b-PMMA acetone (PMMA block selective solvent) was used [37, 45]. After taking out annealed samples they have been left in air for residual solvent evaporation until AFM was performed.
On the other hand, PS-b-PCL films were thermally annealed, using the vacuum oven shown in Figure 5. One group of samples was annealed at 100°C and the other at 120°C, slightly and well above glass transition temperatures of each block respectively. For both cases, samples were kept for 72 h [34, 36].

3.3 EXPERIMENTAL TECHNIQUES

3.3.1 Thermal analysis

The thermal properties of block copolymers have been analysed in terms of thermogravimetric analysis (TGA) and differential scanning calorimetry (DSC). Samples were prepared as follows: a small amount of solution (5 ml for solutions 1 and 2 and 4 ml for solution 3) was put in a cylindric glass container letting the solvent to evaporate, then from the irregular film the necessary amount of polymer was collected and grinded.

3.3.1.1 TGA

By this technique, the mass variation of the sample is measured during heating process. It is mostly used for polymers, so a mass loss due to the degradation of the material usually occurs. Under certain conditions (oxidizing atmosphere and low heat rate for instance) a slight mass gain may be measured. During heating the mass loss is not only due to the degradation of the sample but also to moisture and residual solvent evaporation. Depending on the temperature ramp there are different TGAs such as controlled rate TGA, stepwise TGA, modulated TGA and so on. An important factor to consider in this technique is the atmosphere, which plays a fundamental role by establishing the temperature range in which the degradation reaction (and so the mass loss) takes place. Usually the atmosphere is air or nitrogen, but it may vary depending on the material and application. The output of the analysis is the mass loss (usually expressed in percentage of initial mass) related to temperature (integral curve), whilst with its derivative the mass loss rate may be evaluated.

The heart of the equipment is the thermobalance, which measures the mass of the sample during all the analysis. Its precision, for a standard model, is around mg^{-4} [46], so there are many factors that to be considered when the results are evaluated, such as buoyancy forces, atmospheric turbulence and electrostatic or magnetic forces that may affect results. They may be managed either by designing the equipment correctly or by considering their influence with a software. The other main components of TGA are the thermocouples, which measure the temperature in the chamber, affected by different factors, like heating rate, thermal conductivity, the enthalpy of reactions and the eventual presence of dust.

In this technique some points are particularly interesting, such as the T on which mass loss starts, the maximum of mass loss rate and the residual mass after degradation. Unfortunately, it is not easy to analyse the kinetics of degradation, because, due to the temperature ramp, there is not enough time to reach equilibrium. For a deeper study of degradation process, once the temperature of degradation is found, the

temperature should be kept constant, so a more detailed speech of the kinetics of reaction may be obtained.
If this technique is combined with another one (for example a GCMS or an IR spectroscopy) it is possible to obtain not only quantitative information, but also qualitative; identifying and characterizing the species obtained after degradation [47].

Thermal analysis (both TGA and DSC) were performed with a Mettler Toledo TGA/DSC3+, shown in Figure 19.

Figure 19. Experimental set up used for thermal analysis

TGA tests were carried out from room temperature to 800°C for PS-b-P4VP and PS-b-PCL samples, from room temperature to 600°C for PS-b-PMMA; while For all tests a heating rate of 10°C/min was used.

3.3.1.2 DSC

In the differential scanning calorimetry, a quantitative calorimetric information of the material subjected to a controlled heating process is obtained. It compares the heat flux necessary to take the sample to a determined temperature with that needed to heat up the reference sample to that temperature. To perform this comparison the temperature difference between the sample and reference is measured. There are two types of DSCs currently used: heat flux (most common) and power compensation.

In heat flux DSC usually the sample and reference are placed in the same chamber and heat is applied. With a thermocouple temperature difference is measured and

the heat flows from the hotter sample to the colder through a leak bridge (often is a disk). With the *ΔT* known and the thermal resistance of the disk too, it is easy to calculate the heat flux with the thermal equivalent of Ohm's Law, as follows.

$$\dot{Q} = \frac{\Delta T}{R}$$

Where ΔT is measured by the thermocouple, R is a function of the material.

In power compensation DSC the sample and the reference are held in two separate chambers, each one equipped with its heater and sensor. Here the temperature of both samples should be the same which is set by the operator, to reach the equilibrium the instrument heats one chamber or the other. The supplied power for balance the temperature between sample and reference is then displayed.

In both cases the analysis is performed in a controlled atmosphere, whose composition is maintained constant thanks to a stream of purge gas; which usually is nitrogen. With this technique important parameters and temperatures may be quickly obtained. Melting temperature, glass transition and crystallization temperature are the most common ones. Moreover, it is also possible to determine the crystallinity degree of samples. The most important parameters are heating rate and the mass of the sample. Varying their value, it is possible to increase the resolution and sensitivity of the analysis, adapting them to the investigation. Another important parameter is the cooling time, which may affect the microstructure of the sample [47]. In this work DSC was performed with the same instrument of TGA. Tests were performed from room temperature to 200°C with a heating rate of 10°C/min. In order to be sure of the reliability of results, one preliminary heating was performed, followed by a cooling step and a second heating ramp. In the following plots just the second heating ramp will be represented.

3.3.2 Morphological analysis by AFM

Atomic force microscopy provides a high-resolution image of the surface topography of the sample. This technique is based on the force which acts between the tip of the probe and the atoms of the surface. The force between the tip and the surface is due to Van der Waals forces and its value is between 10^{-9} and 10^{-6} N. The 100 Å diameter tip is located at the end of a cantilever which is deflected by the forces acting on the tip. The deflection is measured by optical methods, and a 3-D map of the surface may be obtained. The instrument may reach a 5 nm lateral and 0.1 nm vertical resolution, so it perfectly fits with surface analysis of nanostructures like BCPs thin films.

The most common AFM modes are the contact mode, the non-contact mode and the tapping mode. In contact mode repulsive forces act on the tip and it is the most common one thanks to the high resolution possible. On other hand the surface of the sample may be scratched or damaged, so it is not suggested for fragile or soft samples.

In non-contact mode the tip is attracted by the surface of the sample. However, in this case the force acting on the tip is considerably weaker, so the images may be distorted by the contaminant absorbed layer (water vapour, nitrogen) which may be thicker than the distance at which VdW forces act. In tapping mode, the tip is alternatively placed in contact with the surface and lifted during the scanning of the sample. This solution gives best results either in terms of resolution or avoiding damages to the surface. The atmosphere may be ultra-high vacuum, but many instruments operate in air or liquids [48].

Figure 20. A picture of the AFM equipment used in this work. On the left the whole instrument, on the right a zoom of the sample holder and the tip.

this work surface morphologies obtained for different films were studied by atomic force microscopy with a scanning probe microscopy AFM Dimension ICON of Bruker, operating in tapping mode (TM–AFM). An integrated silicon tip/cantilever, from the same manufacturer, having a resonance frequency of around 300 kHz, was used. Measurements were performed at a scan rate of 1 Hz/s, with 512 scan lines.

4 RESULTS AND DISCUSSION

4.1 THERMAL ANALYSIS

4.1.1 PS-bP4VP

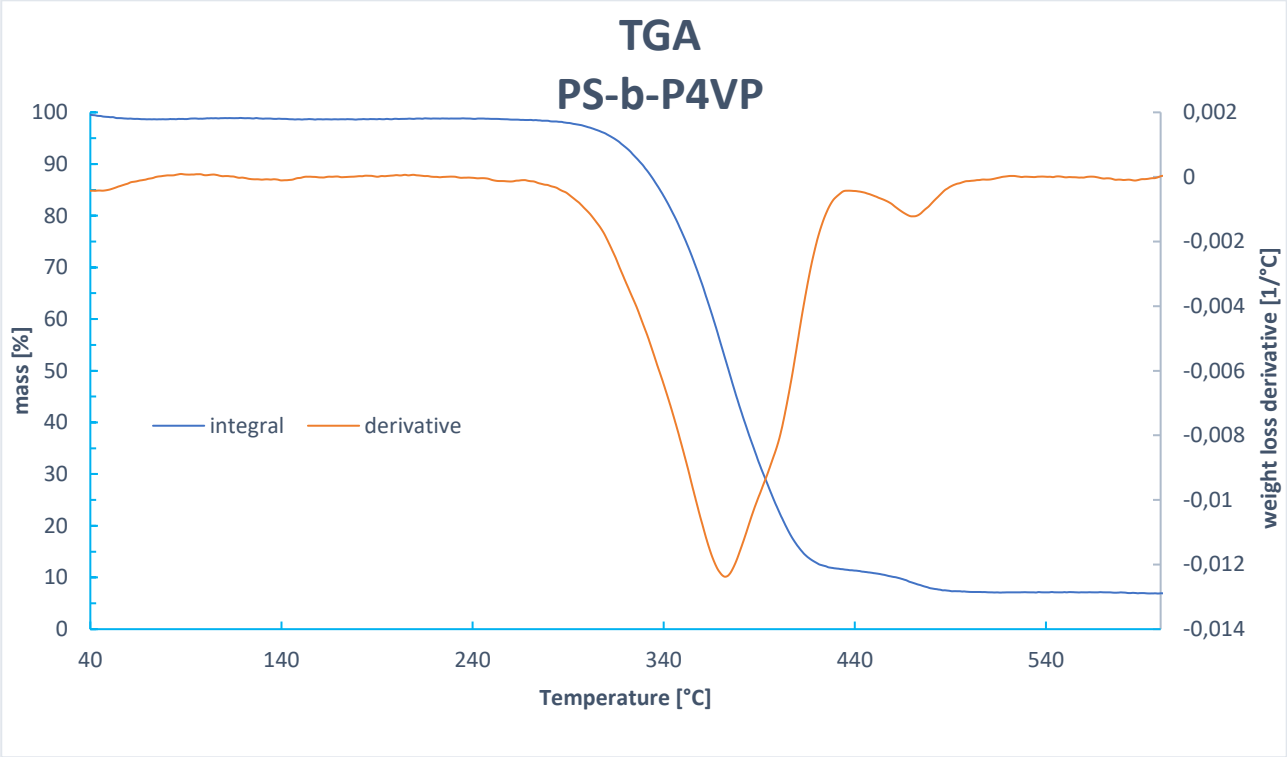

Figure 21. TGA thermograms of PS-b-P4VP block copolymer.

For PS-b-P4VP 1.4038 mg of copolymer were used. From figure 21 it emerges a two-step degradation. Nevertheless in the integral curve this step may seem slight, it is more clear from the derivative curve, were two different peaks (referring to the maximum degradation rate) are clearly seen at around 375°C and 475°C. This behaviour may be explained, according to literature, with the different thermal resistance of two blocks, whose maximum decomposing rate is typically reported around 430°C for PS (M_n=8000) and 400°C for P4VP (M_n=13000) [49]. Therefore, the two steps of degradation may be assigned to P4VP block (the one at around 375°C) and the higher one to PS block.

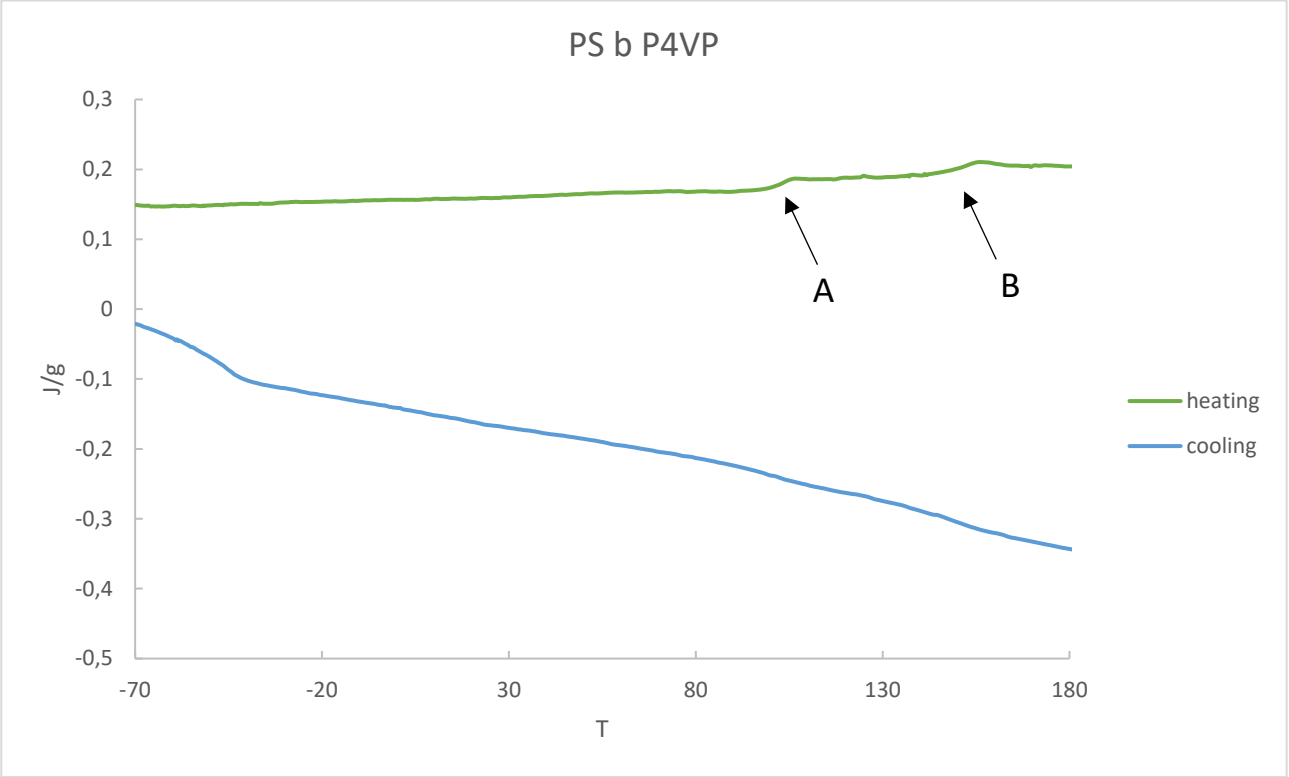

Figure 22 DSC thermograms of PS-b-P4VP block copolymer.

For DSC 2.033 mg of powder were used as sample. As shown in figure 22, in the plot it doesn't appear any appreciable peak, so it is supposed that the two blocks are both amorphous. Following this path, the presence of a T_g is expected. There are two shifts: one at 104°C and one around 149°C point A and B respectively. The presence of two different glass transition temperatures with a value similar to the one of the respective homopolymers (which, according to literature are 100°C and 150°C for PS and P4VP respectively) means that the two blocks must be phase separated, in this case, it confirms the microphase separation.

4.1.2 PS-b-PMMA

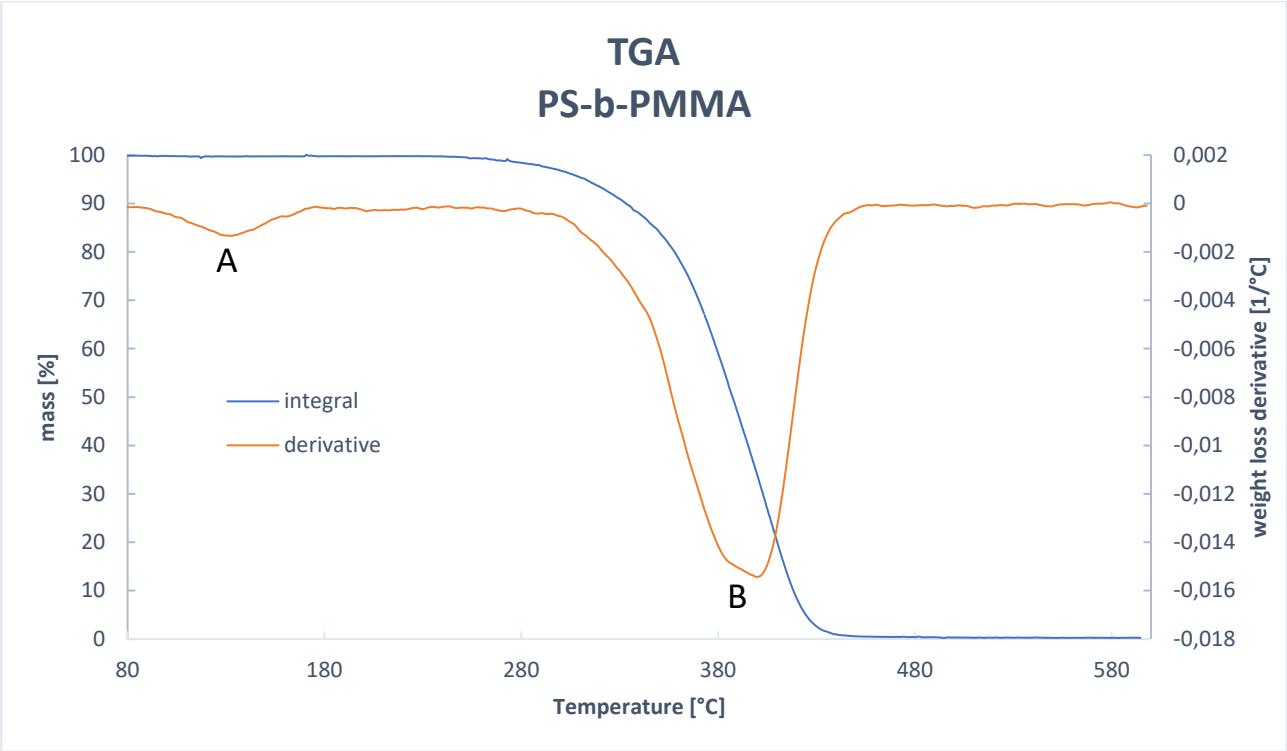

Figure 23. TGA thermograms of PS-b-PMMA block copolymer

For TGA 0.6740 mg of powder were used. From the plot in figure 23 it is possible to see two peaks in the derivative curve, which means two degradation steps. Looking at the temperature interval in which falls the first peak (peak A) it is possible to state that it represents the small mass loss due to the evaporation of the water present in the sample (dehydration). As can be observed in the integral curve it is a slight mass loss, negligible if compared to the mass loss due to thermal degradation, which starts at around 330°C and it reaches the maximum rate at 400°C (point B in the derivative curve). The extrapolated thermal degradation temperature (TDT) may be fixed around 380°C. As shown from the integral curve the degradation of the backbone chain occurs in one single step [50].

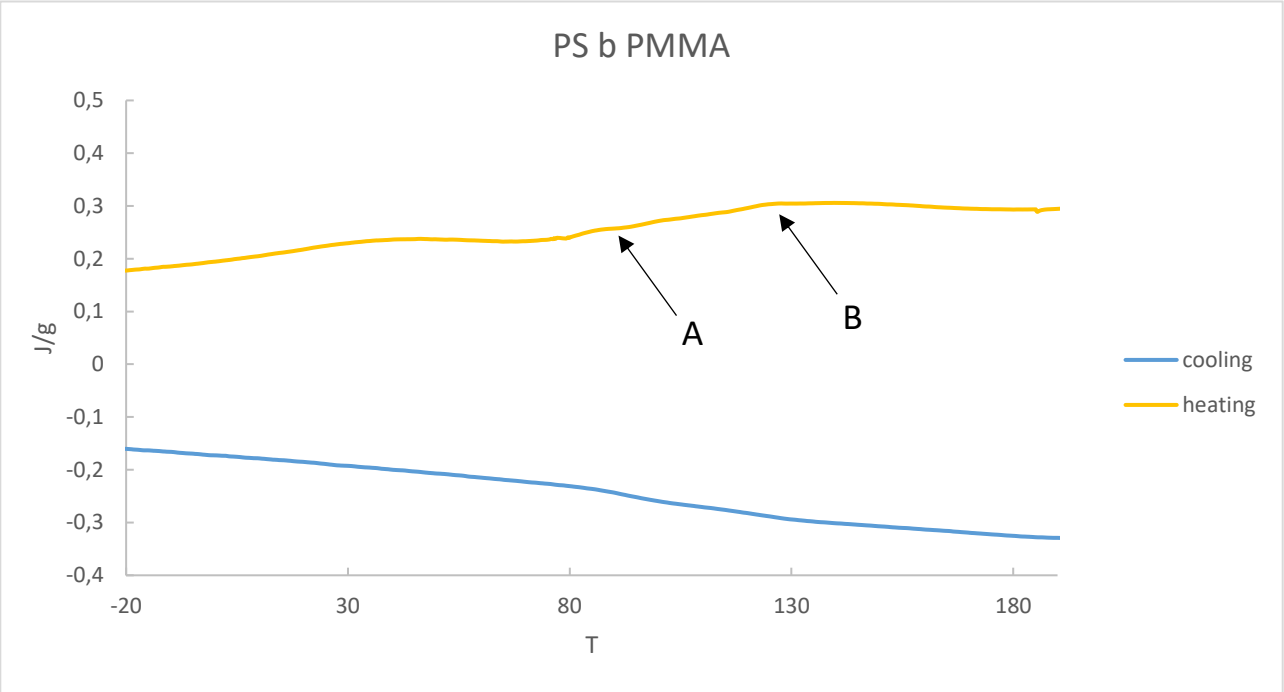

Figure 24 DSC thermograms of PS-b-PMMA copolymer

For DSC 2.34 mg of powder were used. From figure 24 it may be observed that, as for PS-b-P4VP, also this copolymer is totally amorphous. This because neither during the cooling nor during the heating any peak appears, which would represent a crystallization or a melting. The thermogram highlights two shifts (A and B in figure 24) which means two different T_gs, respectively 96°C and 128°C. These values are, according to literature, close to the glass temperatures of single blocks (100°C for PS and 130°C for PMMA) which means, as seen above for the previous copolymer, microphase separation of the two blocks [51].

4.1.3 PS-b-PCL

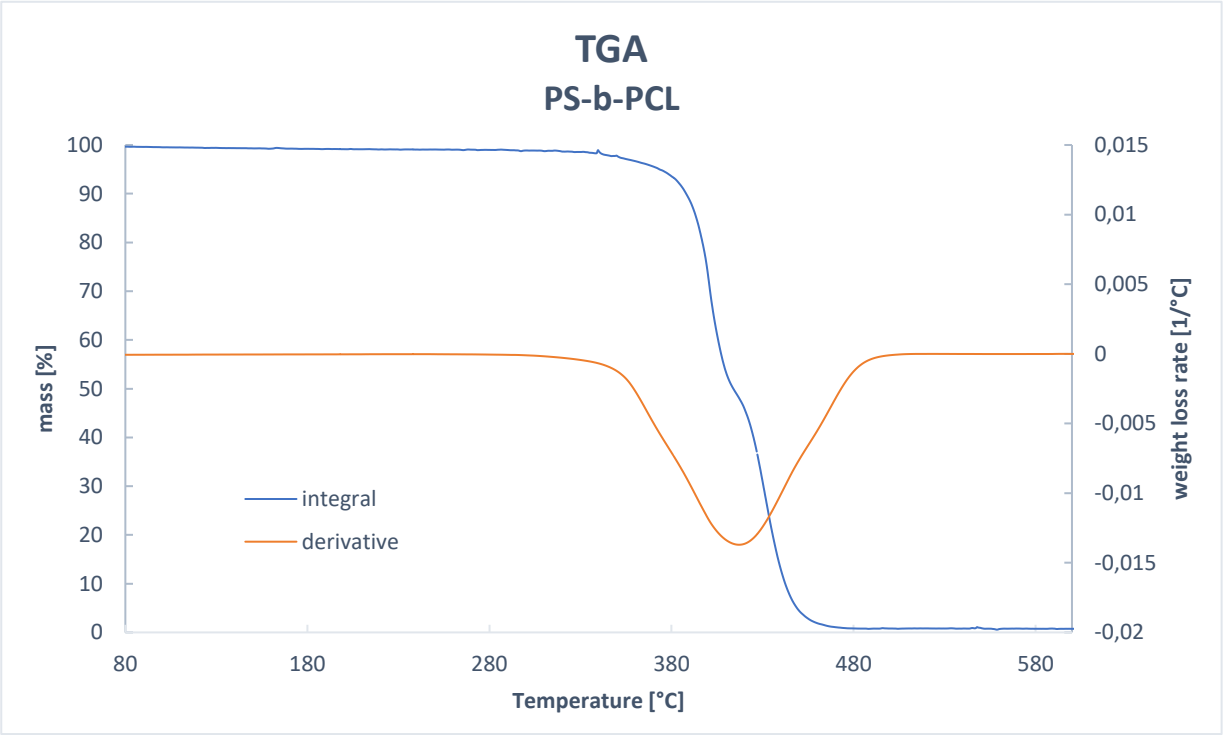

Figure 25 TGA thermograms of PS-b-PCL block copolymer

For TGA test 5.2801 g of powder were used. From the plot in figure 25 it may be observed a single step degradation with a slight shift around 400°C, probably due to the difference of thermal degradation temperature of the two blocks. However, the degradation may be considered as a single step one, observing the derivative curve, which presents a single peak at 417°C.Thermal degradation begins around 380°C.

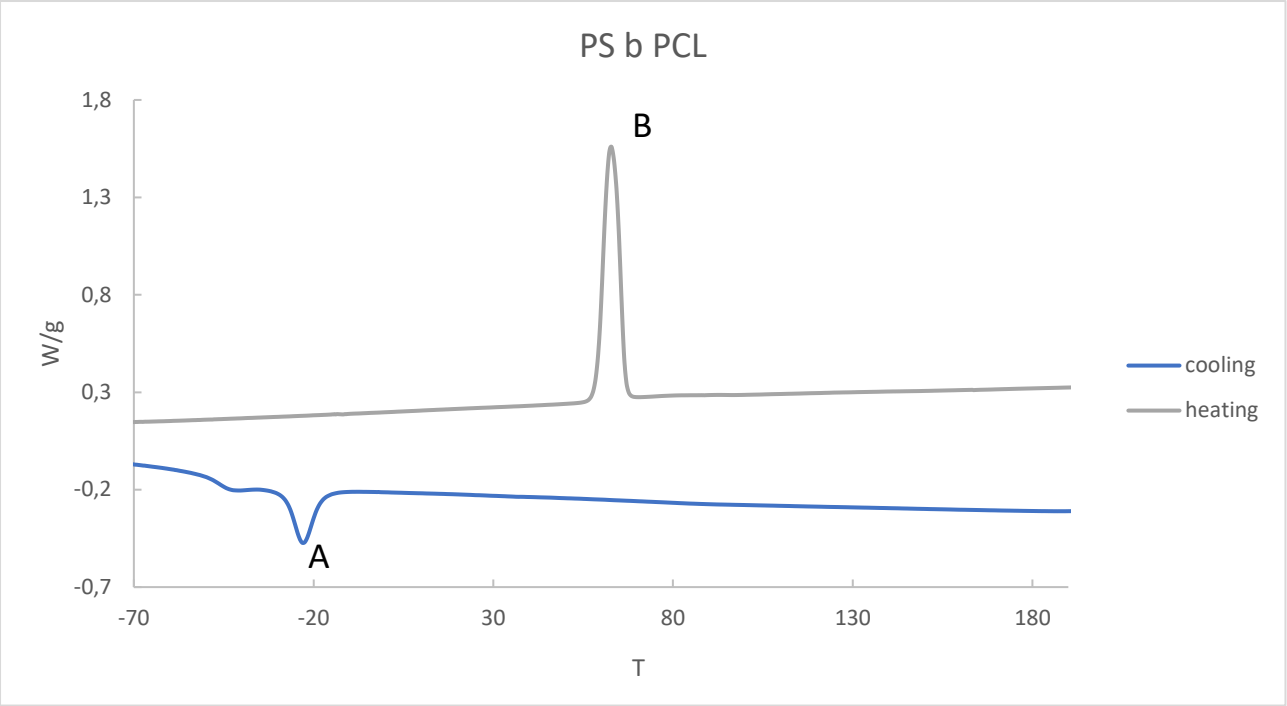

Figure 26 DSC thermograms of PS-b-PCL block copolymer

For the calorimetry 4.81 mg of powder were used. From this analysis it emerges the presence of a crystalline phase, as the presence of the two peaks confirms. In figure 26 Peak A (with a negative value) represents the crystallization of a phase (which occurs at around -23°C), on the other hand, peak B represents the melting of the phase (which occurs around 63°C). According to what found in literature, this crystalline phase may be attributed to PCL block, which, in this case, represents the 30% of the copolymer, and whose the crystalline phase is only 5% [52]. A deepening about this crystalline phase will be made in the next chapter, where the film will be observed with the AFM.

	TDT	Tg	Tm	Tc
PS-b-P4VP	330	104		
	460	149		
PS-b-PMMA	380	96		
		128		
PS-b-PCL	380			-23
			63	

Table 2. Some important temperatures of different BCPs. T_m and T_c represent the temperatures of melting and crystallization respectively. All the values are expressed in °C

4.2 AFM

4.2.1 PS-b-P4VP

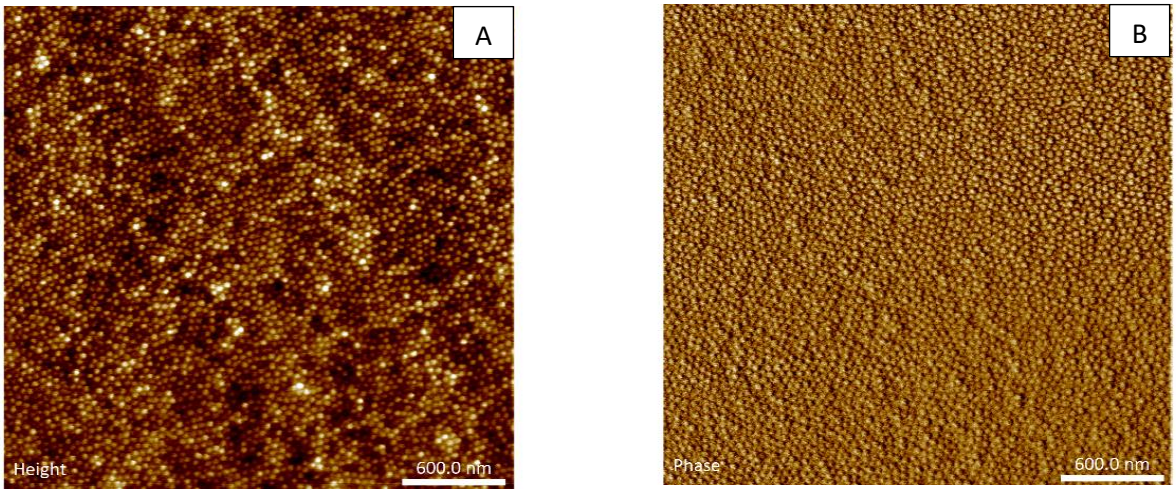

Figure 27. AFM height (A) and phase (B) images of PS-b-P4VP block copolymer after 24h annealing treatment

From figure 27 it is clear an HPC morphology, where cylinders are perpendicular to the surface. It is already possible to distinguish some stripes, especially in image B, which may be a clue on what will happen for longer exposure time.

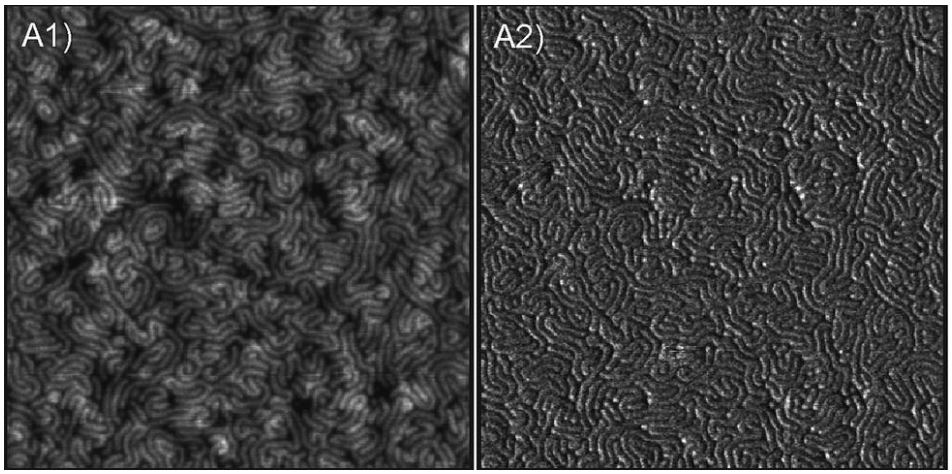

Figure 28. AFM height (A1) and phase (A2) images of PS-b-P4VP block copolymer after 48h annealing treatment

With longer exposure time to dioxane vapours (which is a selective solvent for PS block) a lamellar morphology is reached (shown in figure 28). This may be related to the better affinity of PS domains with the atmosphere, so macromolecules tend to diffuse at the surface, however they are slow, so an intermediate stable phase (HPC) is present and it is seen for shorter exposure times [37]. In both cases, domains are

perpendicularly aligned to the surface, which may underline a certain affinity of both blocks either with the substrate or with the atmosphere.

Either after 24h or 48h annealing treatment a morphology perpendicular to the substrate was obtained, so probably glass may be considered a neutral substrate for this BCP.

4.2.2 PS-b-PMMA

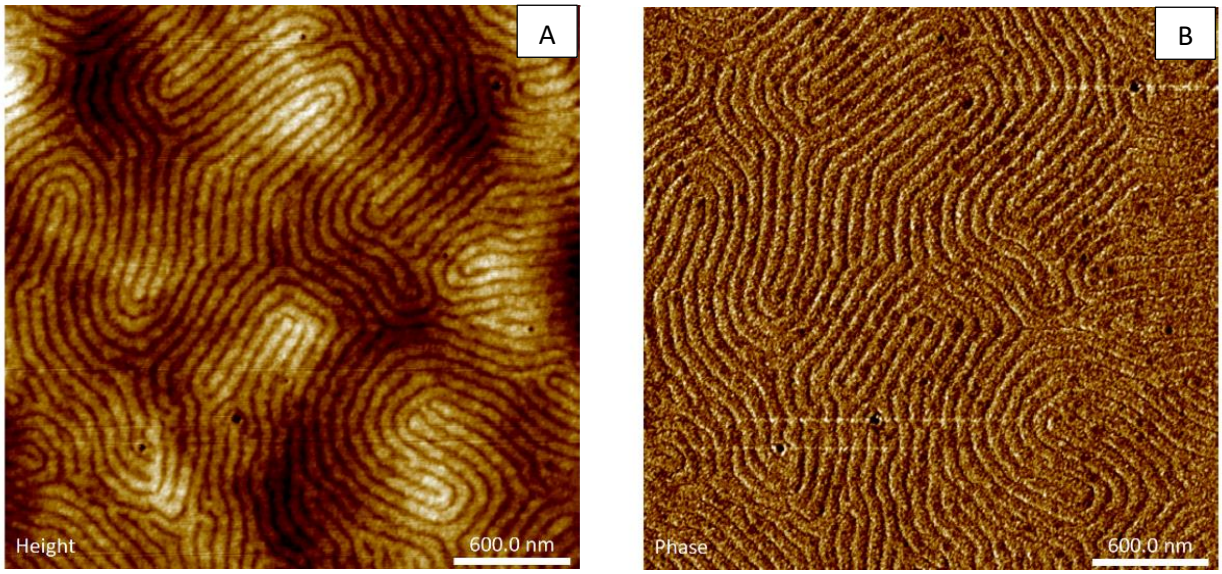

Figure 29. AFM height (A) and phase (B) images of PS-b-PMMA block copolymer after 24 hours annealing treatment

From both images, after only 24 h a stable, well ordered lamellar morphology normal to the surface was observed; with an average interlamellar distance of 77nm. In this case PS and PMMA lamellae are 68 nm and 8 nm wide respectively. As it may be evinced from the height image (figure 29A) the surface of the as spun film is not regular, but darker and brighter regions appear, which means irregular thickness of the film for different regions. From figure 29B a clear lamellar structure may be recognized, where brighter domains are PMMA blocks, while darker ones are PS domains. This is due to the difference in the bulk elastic modulus of the two blocks (typically 3.0 GPa for PS against 3.3 GPa of PMMA), which affects the tapping of the cantilever during the test [53]. After spin coating PMMA seems to be placed at the interface with the substrate, whereas PS block is placed at the surface. During the annealing treatment, thanks to its better affinity with acetone, PMMA chains start swelling and moving to the surface, giving this morphology.

4.2.3 PS-b-PCL

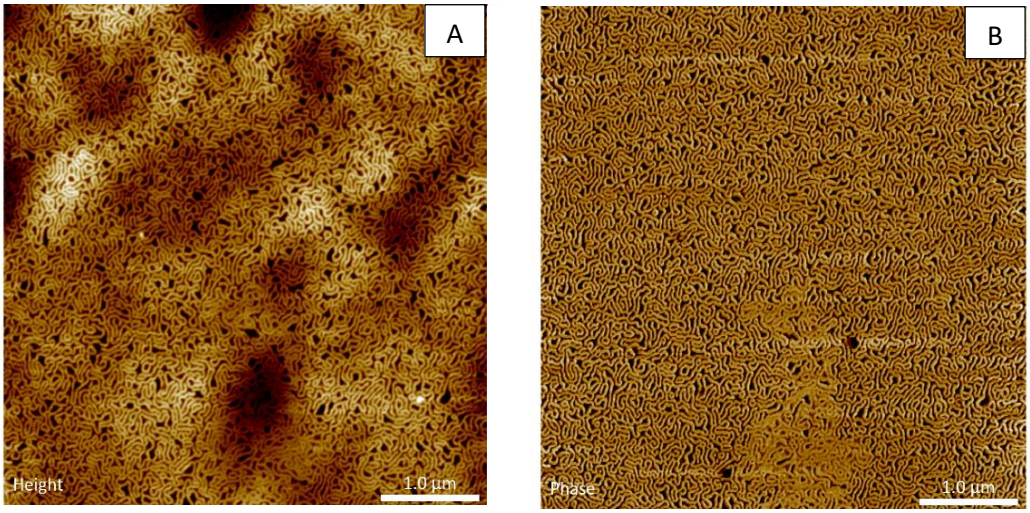

Figure 30. AFM height (A) and phase (B) of PS-b-PCL block copolymer after 100°C annealing treatment

After a 100°C thermal treatment a worm-like morphology was achieved, where brighter domains represent PS block, the hardest phase. However, it may not be considered a high ordered structure.

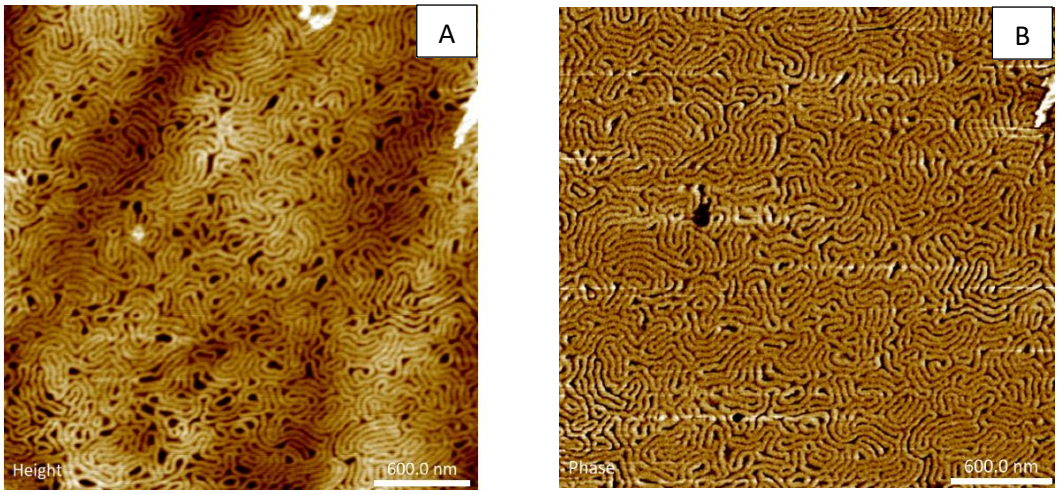

Figure 31. AFM height (A) and phase (B) of PS-b-PCL block copolymer after 120°C annealing treatment

As shown in figure 31 with a higher temperature of annealing (further from the T_g of both blocks) the BCP may reach a more ordered lamellar structure, where lamellae are normal to the surface. This phenomenon is explained with the major mobility of chains, because of the higher temperature.

It is worth to mention that, in both cases, PCL crystalline domains are not observed. Even if in DSC analysis their existence has been proved, they are not visible, because the crystallization degree of PCL block was below 5% in both cases, while PCL represents just 30% of the copolymer

5 CONCLUSIONS

In this work BCPs thin films have been characterized. Thanks to their tuneable morphological properties, these films may be useful for many potential applications in great relevance fields, spreading from medicine to the production of micro-electronical devices. In order to understand how their structure could be tuned, it is fundamental the characterization of BCPs by different techniques, for controlling the entire ordering process that leads to the desired structure.

As demonstrated from the results (chapter 3 section 1), thermal properties of BCP thin films are very similar to those of the homopolymer whose blocks form the copolymer. This fact may be seen from the values of $T_g s$ and *TDT*, which are very similar to those of the single blocks.

As seen from TGA the combination of two different monomers in a single chain doesn't improve thermal properties.

Analysing these results, it is evident that the most technologically interesting feature of these materials is their structure, which results nano ordered.

From AFM images it emerges the importance of annealing treatments for reaching a nanostructure, and, in case of thermal annealing, T_g and the TDT values give the temperature interval of the annealing process itself. In this sense a deeper knowledge of thermal behaviour of the copolymer may lead to a better control in the self-assembling process. On the other hand, for solvent annealing the understanding of both chemical and interfacial interactions between each block and the surface or substrate plays a key role to obtain an ordered structure.

As proven by AFM images nanostructured materials may be easily obtained, with the precision of tens of nm. Opposite to what happens with machinery it is possible to obtain objects with great accuracy without loss of material. Finding the right combination of parameters gives rise to many different structures with many different geometries, making this class of materials very interesting for future applications. The versatility of BCPs for self-assemble into different tuneable nanostructures has been probed in this work for different copolymers.

In this sense this work should be considered as a starting point for further and deeper research, which may lead to astonishing results.

6 REFERENCES

[1] Bates FS, Fredrickson GH. Block copolymers-designer soft materials. Physics Today 52, 2, 32 (1999); DOI: 10.1063/1.882522

[2] Hongbo Feng, Xinyi Lu, Weiyu Wang, Nam-Goo Kang and Jimmy W. Mays. Block Copolymers: Synthesis, Self-Assembly and Applications. A review. 9/10/2017

[3] Hamley IW. Encyclopedia of Polymer Science and Technology. Wiley & sons. 2002. 457-482.

[4] Galder Kortaberria (May 10th2017). Nanostructured Morphologies by Self-Assembly of Diblock Copolymers: A Review, Molecular Self-assembly in Nanoscience and Nanotechnology, Ayben Kilislioğlu and Selcan Karakuş, IntechOpen, DOI: 10.5772/intechopen.68476

[5] Carlos Drummond and Juan Rodriguez-Hernandez. Nonconventional Methods for Patterning Polymer Surfaces. Polymer Surfaces in Motion. Springer International Publishing Switzerland 2015. DOI 10.1007/978-3-319-17431-0_1

[6] Hamley IW. The Physics of Block Copolymers. Oxford University Press, Oxford, UK. 1999.

[7] S.B. Darling. Directing the self-assembly of block copolymers. Science Direct. 02/06/2007

[8] E. Helfand, *Macromolecules* **8**, 552 (1975).

[9] E. Helfand and Z. R. Wasserman, *Macromolecules* **9**, 879 (1976).

[10] Matsen MW, Schick M. Stable and unstable phases of a diblock copolymer melt. Physical Review Leters. 1994;72:2660–2663. DOI: 10.1103/PhysRevLett.72.2660

[11] M. W. Matsen and F. S. Bates, *Macromolecules* **29**, 1091 (1996).

[12] Kim, K.; Schulze, M.W.; Arora, A.; Lewis, R.M.; Hillmyer, M.A.; Dorfman, K.D.; Bates, F.S. Thermal processing of diblock copolymer melts mimics metallurgy. *Science* **2017**, *356*, 520–523

[13] Gohy JF. () Block Copolymer Micelles. In: Abetz V. (eds) Block Copolymers II. Advances in Polymer Science, vol 190. Springer, Berlin, Heidelberg

[14] Thomas P. Russell, G. Coulon, V. R. Deline, and D. C. Miller *Macromolecules* **1989** *22* (12), 4600-4606 DOI: 10.1021/ma00202a036

[15] Fredrickson GH. 1987. Macromolecules 20:2535

[16] Fasolka, M. J., and Mayes, A. M., *Annu. Rev. Mater. Res.* (2001) **31**, 323

[17] Julie N. L. Albert and Thomas H. Epps. Self-assembly of block copolymer thin films. Materials today. Volume 13, Issue 6, June 2010, 24-33

[18] Ponsinet, Virginie. (2015). Nanopatterns Produced by Directed Self-Assembly in Block Copolymer Thin Films. 10.1007/978-3-319-17431-0_4.

[19] Charles T. Black, Christopher Forrey, Kevin G. Yager. Thickness-Dependence of Block Copolymer Coarsening Kinetics. Submitted to Soft Matter. March 2017

[20] Krausch, G. and Magerle, R. (2002), Nanostructured Thin Films via Self-Assembly of Block Copolymers. Adv. Mater., 14: 1579-1583. doi:10.1002/1521-4095(20021104)14:21<1579::AID-ADMA1579>3.0.CO;2-6

[21] Gu, Xiaodan, "Self-Assembly of Block Copolymers by Solvent Vapor Annealing, Mechanism and Lithographic Applications" (2014).
Doctoral Dissertations. 7.

[22] Mohamed, LOUCIF SEIAD & K. MKuppuswamy, V & Ferhat, Marhoun & Gronheid, R. (2018). Template Optimization of Block Copolymer Thin Films by Self-Assembly Process. 10.1007/978-3-319-89707-3_19.

[23] Salvatore S. (2015) Gyroid Metamaterial Fabrication. In: Optical Metamaterials by Block Copolymer Self-Assembly. Springer Theses (Recognizing Outstanding Ph.D. Research). Springer, Cham

[24] F Ferrarese Lupi, T J Giammaria, M Ceresoli, G Seguini, K Sparnacci, D Antonioli, V Gianotti, M Laus and M Perego. Rapid thermal processing of self-assembling block copolymer thin films. Nanotechnology 24 (2013) 315601

[25] Dong Hyun Lee, Heesook Cho, Seungmin Yoo, Soojin Park, Ordering evolution of block copolymer thin films upon solvent-annealing process, Journal of Colloid and Interface Science, Volume 383, Issue 1, 2012, doi.org/10.1016/j.jcis.2012.06.030.

[26] Christophe Sinturel, Marylène Vayer, Michael Morris, Marc A. Hillmyer. Solvent Vapor Annealing of Block Polymer Thin Films. *Macromolecules*201346145399-5415 Publication Date:June 28, 2013 doi.org/10.1021/ma400735a

[27] Siao-Wei Yeh and Kung-Hwa Wei, Ya-Sen Sun, U-Ser Jeng, and Keng S. Liang, CdS Nanoparticles Induce a Morphological Transformation of Poly(styrene-b-4-vinylpyridine) from Hexagonally Packed Cylinders to a Lamellar Structure, Macromolecules 2005, 38, 6559-6565

[28] Hernán E. Romeo, Ileana A. Zucchi, Maite Rico, Cristina E. Hoppe, Roberto J. J. Williams, Macromolecules201346124854-4861Publication Date:June 4, 2013

[29] Marco Sangermano, slides of nanostructured materials course, Politecnico of Torino, a.y. 2018-2019

[30] Luo. Directed Block Copolymer Thin Film Self-Assembly: Emerging Trends Nanopattern Fabrication. Macromolecules 46(19):7567-7579. American Chemical Society 2013 0024-9297

[31] Youn Kim, So & A. Register, Richard. (2013). Applications of Block Copolymers in Thin Films: Nanopatterning. 10.1007/978-3-642-36199-9_63-1.

[32] Hamley, Ian. (2009). Ordering in thin films of block copolymers: Fundamentals to potential applications. PROGRESS IN POLYMER SCIENCE. 34. 1161-1210. 10.1016/j.progpolymsci.2009.06.003.

[33] De Rosa, Claudio Diletto, Claudia Auriemma, F. De Ballesteros, O.R. Di Girolamo, Rocco Morvillo, Pasquale. (2014). Sviluppo di nanocompositi a base di copolimeri a blocchi per celle fotovoltaiche organiche.

[34] Polymerdatabase.com

[35] chemicalbook.com

[36] Laurence McKeen; 13 - Renewable Resource and Biodegradable Polymers; Laurence McKeen; In Plastics Design Library; The Effect of Sterilization Methods on Plastics and Elastomers (Fourth Edition); William Andrew Publishing; 2018; pp417-435

[37] Barandiaran, Irati & Kortaberria, Galder. (2015). Synthesis and characterization of nanostructured PS-b-P4VP/Fe2O3 thin films with magnetic properties prepared by solvent vapor annealing. RSC Advances. 5. 10.1039/C5RA21477G.

[38] D.W. van Krevelen Klaas te Nijenhuis; Properties of Polymers; 4th Edition; Elsevier Science; 9th February 2009

[39] Guaita, Ciardelli, La Mantia, Pedemonte; Fondamenti di scienza dei polimeri; Ed. Nuova Cultura; 2006

[40] O'Driscoll, S. , Demirel, G. , Farrell, R. A., Fitzgerald, T. G., O'Mahony, C. , Holmes, J. D. and Morris, M. A. (2011), The morphology and structure of PS-b-P4VP block copolymer films by solvent annealing: effect of the solvent parameter. Polym. Adv. Technol., 22: 915-923. doi:10.1002/pat.1596

[41] Barton, Allan F. M. Crc Handbook of Polymer-Liquid Interaction Parameters and Solubility Parameters. Boca Ratón, Florida: CRC Press, 1990.

[42] Allan F. M. Barton Chemical Reviews 1975 75 (6), 731-753 DOI: 10.1021/cr60298a003

[43] Yu-Chi Lee, Ya-Sen Sun, Jiun-You Liou, Wei-Tsung Chuang, Hierarchically-responded assembly of block copolymer thin films with stimuli of varied solvent selectivity, Polymer, Volume 53, Issue 25, 2012, Pages 5972-5981,

[44] Langmuir2011272314545-14553 Publication Date:September 27, 2011 https://doi.org/10.1021/la203114j

[45] J. Gong, H. Ahn, E. Kim, H. Lee, S. Park, M. Lee, S. Lee, T. Kim, E. Kwak and D. Y. Ryu, Soft Matter, 2012, 8, 3570 DOI: 10.1039/C2SM07262A

[46] https://www.mt.com

[47] Menczel, Prime; Thermal Analysis of Polymers, fundamentals and applications; Copyright © 2009 John Wiley & Sons, Inc.

[48] G. Cicero; Dispense di Fisica delle superfici; Politecnico di Torino; a.y. 2018/2019

[49] Chih-Feng Huang, Shiao-Wei Kuo, Jem-Kun Chen and Feng-Chih Chang; Synthesis and Characterization of Polystyrene-b-Poly(4-vinyl pyridine) Block Copolymers by Atom Transfer Radical Polymerization; January 2005, Journal of Polymer Research 12(6):449-456

[50] G. del C. Pizarro, O. G. Marambio1, M. Jeria-Orell, C. M. González-Henríquez, M. Sarabia-Vallejos, K. E. Geckeler; Effect of annealing and UV-radiation time over micropore architecture of self-assembled block copolymer thin film. eXPRESS Polymer Letters Vol.9, No.6 (2015) 525–535

[51] Chengzhi Chuai, Kristoffer Almdal, Jørgen Lyngaae-Jørgensen; Thermal Behavior and Properties ofPolystyrene/Poly(methyl methacrylate) Blends; Journal of Applied Polymer Science, Vol. 91, 609 – 620 (2004)

[52] Irati Barandiaran, Ariel Cappelletti, Miriam Strumia, Arantxa Eceiza, Galder Kortaberria; Generation of nanocomposites based on (PMMA-b-PCL)-grafted Fe2O3 nanoparticles and PS-b-PCL block copolymer; European Polymer Journal, Elsevier, September 2014

[53] J Gutierrez et al; 2009; Nanotechnology 20 225603